Article

Cell Reports

Neonatal Rhesus Macaques Have Distinct Immune Cell Transcriptional Profiles following HIV Envelope Immunization

Graphical Abstract

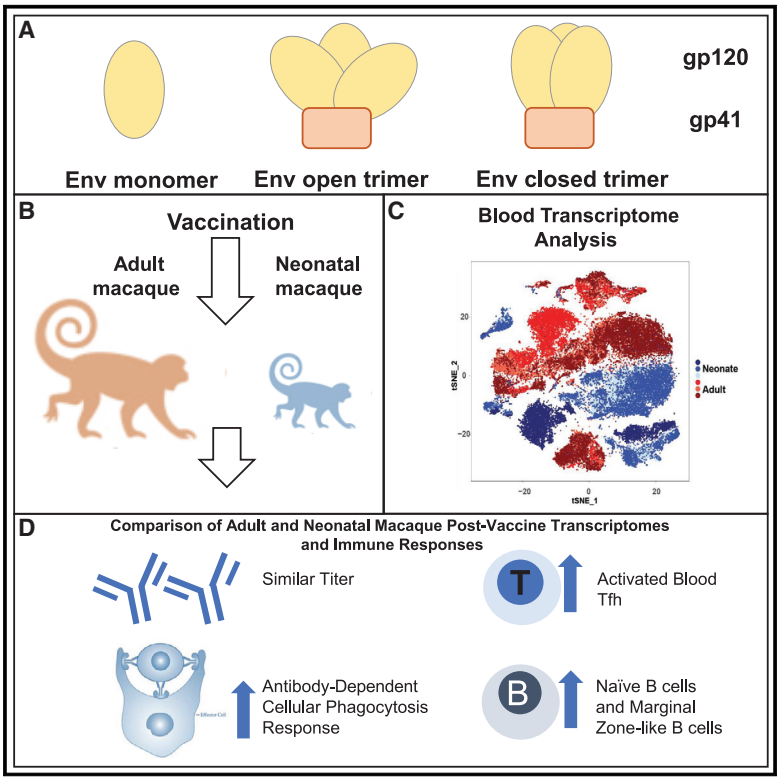

Highlights

- Neonatal immunity to HIV-1 Env immunogens, including soluble trimers (SOSIP)
- Neonatal Env immunity to DNA or protein-based vaccine platforms
- Neonatal immune cells have distinct transcriptome profiles from adults
- Microbial imprinting of the B cell repertoire can occur within a week of birth

Authors

Qifeng Han, Todd Bradley, Wilton B. Williams, ..., Mark G. Lewis, Koen K.A. Van Rompay, Barton F. Haynes

Correspondence

barton.haynes@dm.duke.edu

In Brief

Han et al. demonstrate that infant macaques are capable of responding to HIV vaccines currently studied in human clinical trials. The nature of the neonatal immune system following immunization also suggests a state permissive for generating HIV-1 antibodies. Thus, infant HIV-1 immunization remains a viable strategy to end this pandemic.

Han et al., 2020, Cell Reports *30*, 1553–1569
February 4, 2020
https://doi.org/10.1016/j.celrep.2019.12.091

CellPress

Cell Reports
Article

Neonatal Rhesus Macaques Have Distinct Immune Cell Transcriptional Profiles following HIV Envelope Immunization

Qifeng Han,[1,7] Todd Bradley,[1,7,8] Wilton B. Williams,[1,7] Derek W. Cain,[1] David C. Montefiori,[1] Kevin O. Saunders,[1] Robert J. Parks,[1] Regina W. Edwards,[1] Guido Ferrari,[1] Olaf Mueller,[2] Xiaoying Shen,[1] Kevin J. Wiehe,[1] Steven Reed,[3,10] Christopher B. Fox,[3] Wes Rountree,[1] Nathan A. Vandergrift,[1,9] Yunfei Wang,[1] Laura L. Sutherland,[1] Sampa Santra,[4] M. Anthony Moody,[1] Sallie R. Permar,[1] Georgia D. Tomaras,[1] Mark G. Lewis,[5] Koen K.A. Van Rompay,[6] and Barton F. Haynes[1,11,*]

[1]Duke Human Vaccine Institute, Duke University School of Medicine, Durham, NC, USA
[2]Center for Genomics of Microbial Systems, Duke University Medical Center, Durham, NC, USA
[3]IDRI, Seattle, WA, USA
[4]Center for Virology and Vaccine Research, Beth Israel Deaconess Medical Center, Harvard Medical School, Boston, MA, USA
[5]BIOQUAL, Inc., Rockville, MD, USA
[6]California National Primate Research Center, University of California, Davis, Davis, CA, USA
[7]These authors contributed equally
[8]Present address: Children's Mercy Hospital, Kansas City, MO 64108, USA
[9]Present address: RTI International, Research Triangle Park, NC, USA
[10]Present address: Onc Bio, Seattle, WA 98102, USA
[11]Lead Contact
*Correspondence: barton.haynes@dm.duke.edu
https://doi.org/10.1016/j.celrep.2019.12.091

SUMMARY

HIV-1-infected infants develop broadly neutralizing antibodies (bnAbs) more rapidly than adults, suggesting differences in the neonatal versus adult responses to the HIV-1 envelope (Env). Here, trimeric forms of HIV-1 Env immunogens elicit increased gp120- and gp41-specific antibodies more rapidly in neonatal macaques than adult macaques. Transcriptome analyses of neonatal versus adult immune cells after Env vaccination reveal that neonatal macaques have higher levels of the apoptosis regulator *BCL2* in T cells and lower levels of the immunosuppressive interleukin-10 (IL-10) receptor alpha (*IL10RA*) mRNA transcripts in T cells, B cells, natural killer (NK) cells, and monocytes. In addition, immunized neonatal macaques exhibit increased frequencies of activated blood T follicular helper-like (Tfh) cells compared to adults. Thus, neonatal macaques have transcriptome signatures of decreased immunosuppression and apoptosis compared with adult macaques, providing an immune landscape conducive to early-life immunization prior to sexual debut.

INTRODUCTION

Neonatal immune systems can respond equally well or better than adults to vaccines against several pathogens, including malaria (Bliss et al., 2017), measles (Capozzo et al., 2006), hepatitis B (Ota et al., 2004), and bacillus Calmette-Guérin (BCG) (Vekemans et al., 2001). However, the neonatal response to other vaccines has been reported to be inferior to that of older children (Gans et al., 1998; Gruber et al., 1997; Wright et al., 2000). The immune system of infants and young children has also been shown to be capable of generating vaccine-induced protection against pathogens such as enterovirus 71 (EV71) (Zhu et al., 2014).

While the prenatal environment is relatively sterile compared to that of adults (Neu, 2016; Nguyen et al., 2016), the immune cells of neonates adapt to respond quickly to pathogens (Martinez et al., 2015). However, immune cells of neonates and adults have phenotypic and functional differences due to the immaturity of the neonatal immune system (Adkins et al., 2004; Kollmann et al., 2017; Langrish et al., 2002; Lee et al., 2019; Melvan et al., 2010; PrabhuDas et al., 2011; Siegrist and Aspinall, 2009; Whittaker et al., 2018; Willems et al., 2009; De Wit et al., 2003).

HIV-1 envelope (Env) gp120 immunogens have elicited plasma-binding antibody responses in human and monkey neonates (Cunningham et al., 2001; Fouda et al., 2015; Johnson et al., 2005; Kintu et al., 2013; McFarland et al., 2001, 2006; McGuire et al., 2017; Phillips et al., 2017). Infants vaccinated with the Chiron recombinant HIV-1 gp120 with MF59 adjuvant generated higher immunoglobulin G (IgG) levels against the first and second variable loops (V1V2) than adults, which is important, since V2 antibody responses were associated with reduced risk of HIV-1 acquisition in the RV144 vaccine trial (Fouda et al., 2015; Haynes et al., 2012; McGuire et al., 2017). However, it is unclear if neonates respond as well as adults to well-folded soluble, stabilized HIV-1 Env trimers (Sanders et al., 2013), which have been shown to induce autologous tier 2 neutralizing antibodies in adult rhesus macaques and weak heterologous neutralizing antibodies in rabbits (Havenar-Daughton et al., 2016; Pauthner et al., 2017; Saunders et al., 2017a).

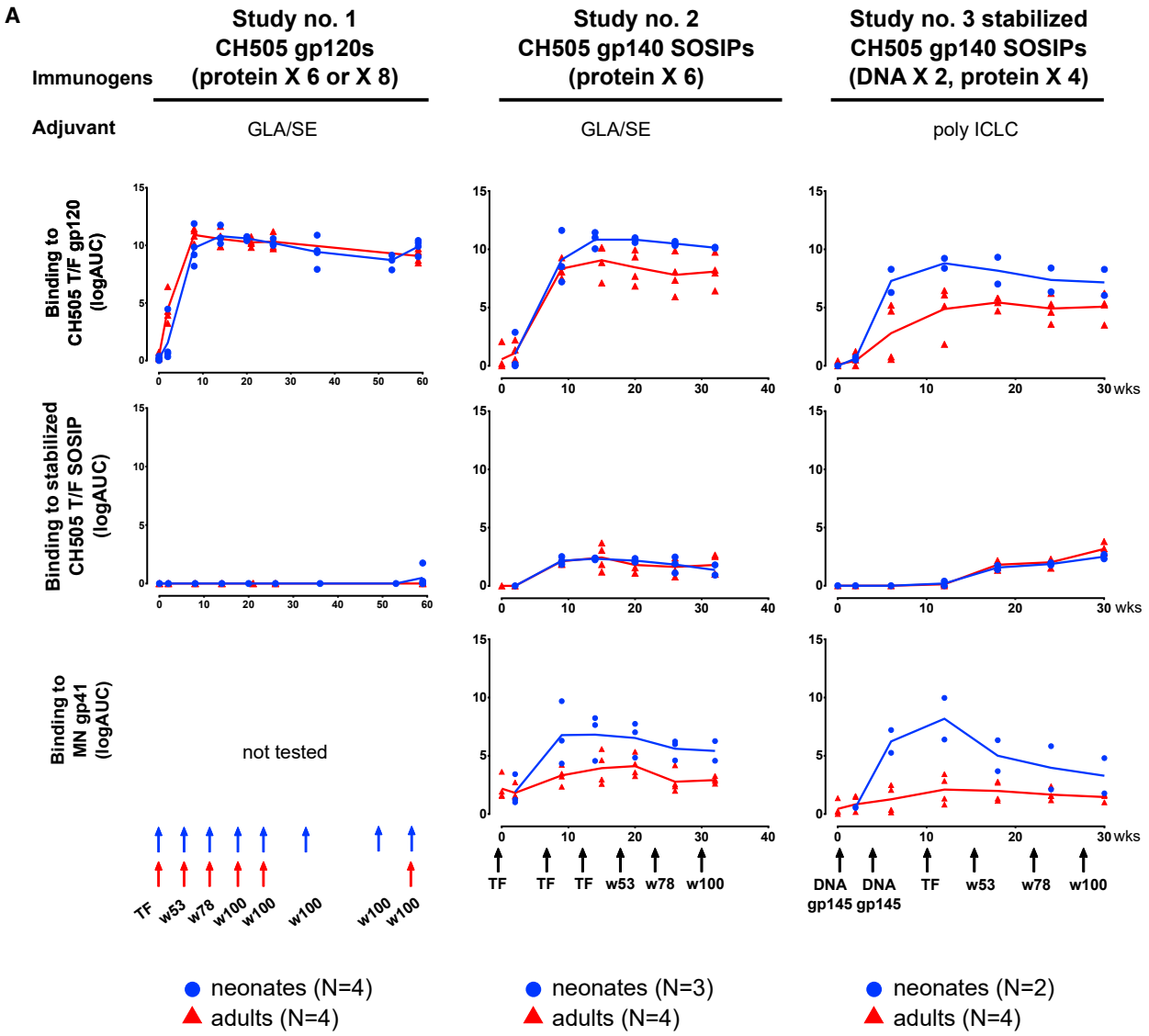

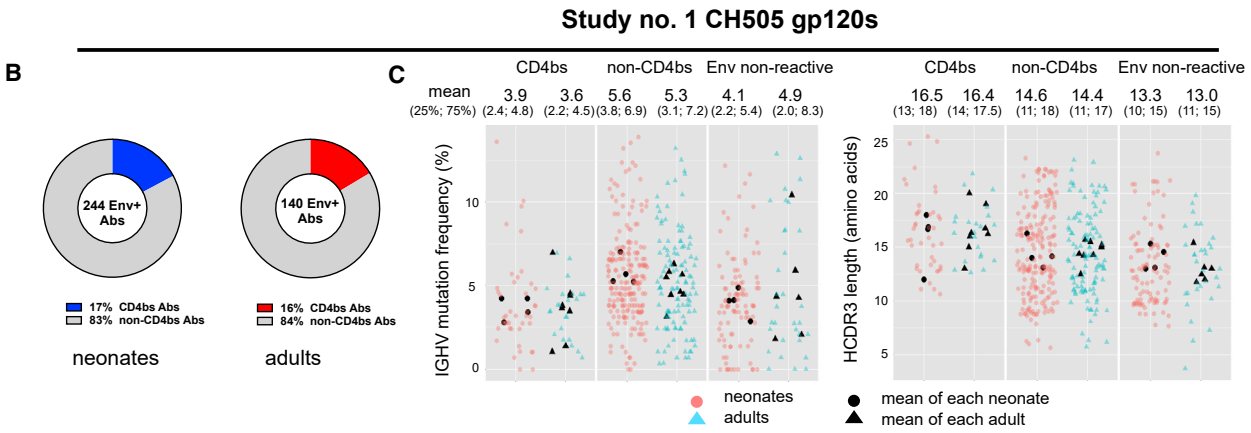

(legend on next page)

To date, broadly neutralizing antibodies (bnAbs) are not consistently elicited following HIV-1 Env vaccination but are generated in ~50% of HIV-1 infected adults only after several years of infection, with accumulation of high levels of antibody mutations (Bonsignori et al., 2017; Doria-Rose et al., 2014; Haynes and Burton, 2017; Hraber et al., 2014; Liao et al., 2013). Recent reports suggest that bnAb induction occurs in HIV-1-infected infants with faster kinetics and lower somatic mutations (Goo et al., 2014; Muenchhoff et al., 2016; Simonich et al., 2016). Thus, if neonatal and pediatric immune systems respond in an accelerated or more permissive manner to Env forms, this may create a window of opportunity between birth and puberty to generate durable immunity to HIV-1 by vaccination with an appropriate Env regimen.

We previously identified sequential Envs associated with the induction and maturation of CD4-binding site (CD4bs) bnAbs in the HIV-1-infected individual CH505 who was followed from early infection to the development of bnAbs (Bonsignori et al., 2016; Gao et al., 2014; Liao et al., 2013). CH505 transmitted-founder (T/F) Env was the first autologous Env found to initiate CD4bs bnAb lineages in humans (Liao et al., 2013), and the CH505 T/F and evolved sequential Env variants have been shown to be immunogenic in bnAb knockin mice and adult macaques (Saunders et al., 2017a; Williams et al., 2017). These CH505 Env variants are being tested in adults in the HIV Vaccine Trials Network (HVTN) 115 trial (https://clinicaltrials.gov identifier NCT03220724), and a trial in neonates is being planned (HVTN 135).

Here, we immunized neonatal and adult macaques with HIV-1 CH505 gp120 or SOSIP trimer immunogens to compare the ability of neonatal and adult macaque immune systems to respond to these Env immunogen forms. We found that immunization of neonatal macaques with trimeric HIV-1 CH505 Envs induced plasma antibody titers that increased more rapidly in neonatal macaques than adult macaques. Increased frequencies of activated circulating T follicular helper-like (Tfh) cells following Env immunization were observed in immunized neonatal macaques compared to adults. Moreover, single-cell transcriptomic analysis of neonatal versus adult blood immune cells showed distinct transcriptomes, with elevated *BCL2* in T cells and lower interleukin-10 (IL-10) receptor alpha (*IL10RA*) transcripts in post-vaccination neonatal T, B, and natural killer (NK) cells and monocytes, suggesting a more permissive immune environment in macaque neonates for initiation of HIV-1 Env B cell lineages.

RESULTS

Vaccine-Induced Antibody Responses to HIV-1 Envs in Macaque Neonates versus Adults

Three groups of neonatal and adult macaques were vaccinated with either HIV-1 CH505 gp120s or CH505 gp140 SOSIP trimers (Saunders et al., 2017a; Williams et al., 2017). The first group of neonatal (N = 4) and adult (N = 4) (Williams et al., 2017) macaques received sequential 4-valent CH505 gp120s (Williams et al., 2017) in the Toll-like receptor 4 (TLR4) agonist adjuvant glucopyranosyl lipid-A (GLA) in a stable, oil-in-water emulsion (GLA-SE) (Seydoux et al., 2018) (study 1) (Figure 1A). The study 1 sequential gp120 regimen is being tested in humans in the HVTN 115 clinical trial (NCT03220724).

The second group of neonatal (N = 3) and adult (N = 4) macaques was immunized with sequential 4-valent CH505 gp140 SOSIP trimers (CH505 SOSIPs) (Saunders et al., 2017a) combined with the TLR4 agonist adjuvant, GLA-SE (study 2) (Figure 1A; Saunders et al., 2017a). CH505 SOSIPs were antigenic for V1V2-glycan, CD4bs, and V3-glycan bnAbs (Saunders et al., 2017a).

The third group of neonatal (N = 2) and adult (N = 4) macaques (study 3) received the sequential CH505 gp140 SOSIP trimer Envs (stabilized CH505 SOSIPs) combined with the TLR3 agonist adjuvant polyinosinic-polycytidylic acid stabilized with polylysine and carboxymethylcellulose (poly-ICLC) (Figure 1A; Saunders et al., 2017a; de Taeye et al., 2015). In study 3, animals also received two priming doses of DNA gp145 expressing CH505 T/F prior to sequential CH505 SOSIPs (Saunders et al., 2017a). Due to the small sample size and similar plasma and cellular immune response profiles within CH505-SOSIP-immunized animals in studies 2 and 3, we combined these groups for select comparisons in neonates versus adults.

In study 1, plasma from neonatal and adult macaques immunized with gp120 Envs bound autologous CH505 T/F gp120 Env at similar average titers and mapped predominantly to the third variable region (V3), C1, loop D, and CD4bs epitopes (Figures 1A, S1A, and S1B). It should be noted that neonates in study 1 immunized with gp120 Envs received two more gp120 vaccines than adults beyond five immunizations, but the animals appeared to be hyperimmunized and did not show rises in titers beyond five immunizations. Thus, the data show similar binding titers to immunizing Env regardless of the extra two immunizations in neonates.

Figure 1. Binding Antibody Responses and Repertoire Analysis of Neonatal and Adult Rhesus Macaques Immunized with CH505 Envs

(A) The kinetics of plasma antibody binding to CH505 T/F gp120, stabilized CH505 T/F SOSIP, and MN gp41 in vaccinated neonatal (blue) and adult (red) rhesus macaques tested by ELISA. Each symbol represents one animal, and the best-fit line represents the mean among each group of animals per vaccine group. The immunogens were sequential CH505 gp120s (study 1), CH505 SOSIPs (study 2), and stabilized CH505 SOSIP Envs (study 3), with adjuvants listed below. PBMCs and plasma were collected at each vaccination and 2 weeks after each vaccination. The arrows represent the time of immunization and sequential immunogens (Transmitted/Founder-TF, week 53, week 78, and week 100) are listed below. Nonparametric analysis of longitudinal data (nparLD) was performed on SOSIP-immunized animals combined in studies 2 and 3 (group by time interaction, $p = 0.038$ for gp120 binding).

(B) Frequency of CD4-binding site (CD4bs) mAbs in total CH505 Env-reactive Abs that were isolated from CH505-gp120s-immunized neonatal and adult rhesus macaques after the fourth immunization.

(C) The IGHV nucleotide mutation frequency (%) and amino acid HCDR3 length of CD4bs mAbs, non-CD4bs mAbs, and HIV-1 Env nonreactive mAbs from CH505-gp120s-immunized neonatal (N = 4) and adult (N = 8) rhesus macaques in study 1 inferred by Cloanalyst software program. This analysis includes four additional adult macaques that recieved sequential CH505 Env vaccine regimens as previously reported (Williams et al., 2017). Each symbol represents one mAb, and the filled symbols (black) represent the mean mutation frequency and HCDR3 length for each rhesus macaque per study. Mean, 25th, and 75th percentile values are listed above the plot.

See also Figure S1.

In neonatal macaques immunized with CH505 SOSIP trimers (studies 2 and 3), we compared the plasma-binding levels across three time points (2 weeks after the first, second, and sixth immunizations) using nonparametric analyses of longitudinal data with time (three time points) and group (neonate versus adult) as factors. We observed a more rapid increase in gp120 antibody responses in neonates over adults that was more striking between weeks 2 and 30 in study 3, compared to study 2, where the difference was only more striking after week 10 (Figure 1A). Due to the small sample size within SOSIP-immunized animals in studies 2 and 3, we could not conduct a stratified statistical analyses and thus combined these groups for comparisons and found a statistically significant increase in plasma binding to gp120 protein in neonates compared with adult macaques based on the group-by-time interaction ($p = 0.038$) (see STAR Methods). Additionally, we found that neonate macaques in studies 2 and 3 generally showed higher levels of plasma gp120 and gp41 antibodies over time compared to adults (Figure 1). That neonates immunized with SOSIP trimers displayed similarly low levels of SOSIP-binding antibodies, but higher gp120 and gp41 responses suggest exposure of immunodominant sites on the trimer *in vivo* following immunization. Alternatively, another explanation for increased gp41 antibody responses in neonates compared to adult macaques may be associated with a more cross-reactive nature of neonate compared to adult B cells (Brezinschek et al., 1997; Mackenzie et al., 1991; Plebani et al., 1993; de Vries et al., 2000a) and that gp41 antibodies have been shown to be cross-reactive (Han et al., 2017; Williams et al., 2015). However, we did not confirm the origin of the gp41 antibody responses that appeared to be higher in neonates than adult macaques.

It was of interest to determine if the B cell repertoires were the same or different in neonates versus adults with gp120 immunogens that are currently in the HVTN 115 clinical trial (NCT03220724). Moreover, CH505 TF Env is planned for testing in human neonates by the HVTN. To compare blood-Env-specific memory B cell repertoires in eight adult macaques that recieved sequential CH505 Env vaccine regimes (Williams et al., 2017) with those in neonatal macaques, in study 1, we evaluated the B cell repertoire in four 4-valent gp120-immunized neonatal macaques after the fourth immunization (week 20) in the sequential Env vaccination regimen using HIV-1 Env-specific single memory B cell sorting with fluorophore-labeled recombinant CH505 transmitted/founder (T/F) gp120 proteins. We found that the mean immunoglobulin (Ig) heavy-chain variable region (IGHV) nucleotide mutation frequencies and heavy-chain CDR3 (HCDR3) lengths of HIV-1 Env-reactive CD4bs and non-CD4bs-targeted monoclonal antibodies (mAbs) from neonatal and adult macaques were not statistically different ($p > 0.05$, exact Wilcoxon test) (Figures 1B and 1C). Thus, after four immunizations in study 1, neonatal and adult antigen-specific B cell repertoires acquired similar levels of somatic mutations with comparable immunoglobulin HCDR3 lengths, suggesting that neonatal macaques have similarly diverse B cell repertoires in response to gp120 Envs as adult macaques.

Plasma from each study of neonatal and adult macaques neutralized tier 1 autologous (CH505 w4.3) and heterologous HIV-1 isolates but did not neutralize the autologous tier 2 CH505 T/F virus (Figure S1C). Plasma from studies 1–3 of neonate and adult rhesus macaques neutralized tier 2 virus B.JR-FL produced in the presence of kifunensine (KIF-JRFL) but did not neutralize wild-type tier 2 JRFL pseudoviruses (Figure 2A), which is similar to the neutralization signature of V3-glycan bnAb precursors (Alam et al., 2017; Bonsignori et al., 2017; Saunders et al., 2017b). V3-glycan types of bnAbs make contact with the highly conserved GDIR motif (Gly324, Asp325, Ile326, and Arg327) at the base of the V3 loop (Garces et al., 2014; Pejchal et al., 2011; Sok et al., 2014) and KIF-JRFL neutralization was abrogated or decreased in all neonate and adult macaque plasmas by the G324A mutation (ADIR) mutation (Figure 2A). Mutating Asp325 and Arg327 in tandem (GAIA) ablated the plasma neutralization of KIF-JRFL in gp120-immunized adults, and as well, in a subset of the SOSIP immunized neonates and adult macaques (Figure 2A). However, KIF-JRFL neutralization was not ablated when Asp325 or Arg327 were mutated individually (Figure 2A).

Since non-neutralizing functional activity of antibodies is involved in protection against HIV-1 infection (Haynes et al., 2012; Barouch et al., 2018), we also compared Fc receptor (FcR)-dependent effector functions of plasma antibodies between neonatal and adult macaques after vaccination, including antibody-dependent cellular phagocytosis (ADCP), which has been correlated with protection in previous preclinical studies (Barouch et al., 2013; Tomaras and Plotkin, 2017), as well as the presence of plasma antibodies capable of binding to HIV-1 CH505-infected cells as an additional correlate of protection (Bradley et al., 2017). SOSIP immunization of neonates in combined studies 2 and 3 had higher ADCP responses to CH505 T/F SOSIP across all time points compared to adult macaques (neonate versus adult $p = 0.002$, nonparametric longitudinal data analysis), whereas the ADCP responses to gp120 were similar between neonatal and adult macaques (neonate versus adult $p = 0.15$, nonparametric longitudinal data analysis) (Figure 2B). Plasma antibody binding to the surface of CH505-virus-infected $CD4^+$ T cells increased more rapidly in CH505-SOSIP-immunized neonatal macaques than adult macaques based on the group-by-time interaction ($p = 0.038$, nonparametric longitudinal data analysis) (Figure 2C).

We have previously described several HIV-1 bnAbs with autoreactive profiles (Haynes et al., 2005b). We tested adult and neonatal plasma binding to autoantigens (Haynes et al., 2005a, 2005b) before and after immunizations. One adult macaque after gp120 immunization (week 59, animal 5,363) was found to be positive for dsDNA antibodies, whereas plasma from all the other adult or neonate macaques was negative (data not shown).

Neonatal and Adult Immune Cells Have Distinct Transcriptomes after HIV-1 Env Immunization

Next, we investigated transcriptome differences between neonatal ($N = 3$) and adult ($N = 3$) study 2 macaque peripheral blood mononuclear cells (PBMCs) at single-cell resolution after two immunizations (week 9) with CH505 SOSIP trimers using single-cell RNA sequencing (scRNA-seq) (Bradley et al., 2018; Zheng et al., 2017). We studied the week 9 time point after two immunizations, because this is the earliest time point when the antibody titers increased to near-peak titers and neonates and adult monkeys started to show differences in Env-binding titers. After filtering low-quality cells, we determined the transcriptomes of 23,040 neonatal and 29,266 adult cells with an average

A

Immunogens — Study no. 1 CH505 gp120s (protein X 6 or X 8)

	neonates				adults			
Animal ID	45423	45404	45405	45425	5362	5363	5551	5553
Bleed Week	59	59	59	59	57	57	57	57
MuLV + Kifunensine	<20	<20	<20	<20	<20	21	20	<20
JR-FL +Kifunensine	48	209	152	602	93	264	225	1013
JR-FL.ADIR.4 +Kifunensine	<20	<20	89	290	<20	<20	<20	<20
JR-FL.GAIR.4 +Kifunensine	66	84	90	146	32	51	160	92
JR-FL.GDAR.2 +Kifunensine	66	85	145	140	65	75	193	520
JR-FL.GDIA.3 +Kifunensine	83	84	220	166	77	84	130	599
JR-FL.GAIA.4 + Kifunensine	43	144	81	114	<20	<20	35	<20

ID50 reciprocal dilutions
<20
20-100
100-1000
1000-10,000

Immunogens — Study no. 2 CH505 gp140 SOSIPs (protein X 6) — Study no. 3 stabilized CH505 gp140 SOSIPs (DNA X 2, protein X 4)

	neonates			adults				neonates		adults			
Animal ID	177890	178951	179059	T270	T274	150129	150799	177715	178122	T241	177811	T243	177850
Bleed Week	32	32	32	32	32	32	32	24	24	24	24	24	24
MuLV + Kifunensine	<100	<50	<100	<20	<20	<20	<20	<20	<20	<20	<20	<20	<20
JR-FL +Kifunensine	1821	133	869	1252	926	82	145	333	676	686	190	692	286
JR-FL.ADIR.4 +Kifunensine	<100	<50	<100	<20	54	<20	<20	<20	<20	<20	<20	<20	<20
JR-FL.GAIR.4 +Kifunensine	430	58	197	236	501	91	97	648	202	160	83	123	43
JR-FL.GDAR.2 +Kifunensine	524	<50	404	285	459	147	170	568	152	337	244	193	47
JR-FL.GDIA.3 +Kifunensine	288	<50	226	194	462	108	114	1358	217	231	82	164	151
JR-FL.GAIA.4 + Kifunensine	<100	<50	<100	<20	82	<20	38	118	46	46	45	60	54

B ADCP

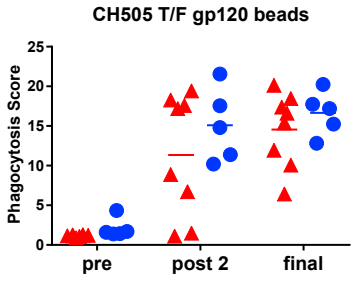

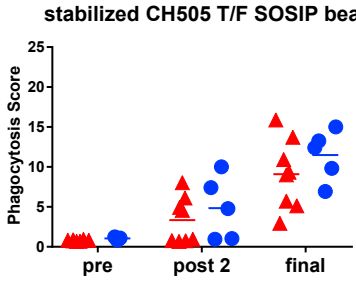

C Binding to infected cells

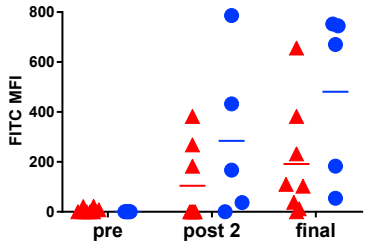

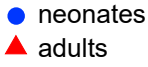

Figure 2. Plasma Neutralizing and Non-neutralizing Functions of Neonatal and Adult Rhesus Macaques Immunized with CH505 Envs

(A) Neutralization profile of plasma from vaccinated neonatal (blue) and adult (red) rhesus macaques via TZM-bl assay studied in each group after six immunizations. Neutralization key is shown on the right. Murine leukemia virus (MuLV) was used as negative virus control.

(B) In CH505 gp140 SOSIPs immunization studies 2 and 3, phagocytosis of CH505 T/F gp120-coated or stabilized CH505 T/F SOSIP-coated beads by THP-1 cells using neonatal and adult macaque plasma before (after the first immunization for neonates due to limited pre-samples) and after the second and sixth immunizations. CH65 and HIVIG were used as negative and positive control antibodies, respectively. Bead phagocytosis was quantified using the phagocytosis score. Horizontal bars are the group mean (average of two replicate experiments).

(C) Plasma titers of antibodies from neonatal and adult macaques that bound to the surface of the CH505-virus-infected $CD4^+$ T (CEM.NKR.CCR5) cell line measured by flow cytometry before (after the first immunization for neonates due to limited pre-samples) and after the second and sixth immunizations. Horizontal bars are the group mean. nparLD was performed on SOSIP-immunized animals combined in studies 2 and 3 ($p = 0.15$ for CH505 T/F gp120 beads group and $p = 0.002$ for stabilized CH505 T/F SOSIP beads group in Figure 2B; $p = 0.038$ for group by time interaction in Figure 2C).

See also Figure S1.

of 56,313 reads per cell and detected a median of 717 genes per cell. Single cells were clustered using graph-based clustering and visualized in two dimensions based on similarity of their transcriptional profiles by an unsupervised machine learning algorithm t-distributed stochastic neighbor embedding (tSNE) (Figure 3A). Cell types that are associated with clusters determined by tSNE were identified using expression of transcript markers enriched in T cells (*CD3D*), B cells (*CD19*, *CD20*), NK cells (*NCR1*), and monocytes (*CD14, LYZ*) (Figures 3B and S2). Using this approach, we found that immune cell subsets in PBMCs from neonatal macaques clustered together and distinct from the immune cell subsets from the adult macaques.

We determined differentially expressed (DE) transcripts using a likelihood ratio test (McDavid et al., 2013) for neonatal immune cells compared to adults (all subsets [ALL] combined, 277 DE genes; Table S1), B cells (360 DE genes; Table S2), T cells (300 DE genes; Table S3), NK cells (428 DE genes; Table S4), and monocytes (623 DE genes; Table S5). We found that 97 DE transcripts were common in all four neonatal immune cell subsets with 68, 42, 113, and 318 DE transcripts unique to B, T, NK, and monocyte cell populations, respectively (Figure 3C). The 97 DE transcripts common in all four neonatal immune cell subsets were enriched for genes involved in the actin cytoskeleton (*ACTB*) (Figures 3D and 3E) and cell movement, RNA splicing, and other immune functions, such as interferon response (*IFITM1* and *IRF3*) (Figures 3D and 3E), suggesting that these transcripts are hallmarks of neonatal immunity in T, B, and NK cells and monocytes.

DE genes related to immune tolerance (*BCL2*, *CD22*, *CD40*, *CD72*, *IL10RA*, *CD86*, *PIK3R1*, *PRKACA*, *TNFSF13*, *IL2RB*, and *TGFB1*) in different cell subsets were also identified (Table S6). Notably, *BLC2* that encodes an integral anti-apoptotic protein in lymphocytes was upregulated and the transcript that encodes *IL10RA* was downregulated in neonatal lymphocytes compared to adult macaque T, B, and NK cells and monocytes (Figure 3E; Table S6). This supports the hypothesis of decreased regulation of immune cell apoptosis in Env-induced neonate immune responses compared to adult macaques. Overall, these data raise the hypothesis that neonatal immune cells were more primed for activation, cellular trafficking, and decreased apoptosis in the context of immune responses.

Neonate B Cells Had Upregulated Marginal Zone (MZ) and Lymphocyte Activation Transcripts

In PBMCs, neonatal and adult macaque B cells that expressed CD19 (*CD19*) and/or CD20 (*MS4A1*) transcripts were re-interrogated by performing tSNE unsupervised clustering to identify differences in study 2 neonate and adult B cells after two immunizations (week 9) (Figure 4A). This resulted in 5,131 and 3,910 neonate and adult B cells, respectively, that clustered in two distinct groups based on their cellular transcriptomes. The 68 DE transcripts unique to B cells included 55 upregulated and 13 downregulated transcripts in neonatal B cells that did not overlap with other immune cell subsets (Figure 4A; Table S2). Transcripts upregulated in neonatal B cells were associated with B cell receptor activation and proliferation and antigen presentation, suggesting a more activated state of B cells in neonates (Figure 4B). Examples of markers that have been associated with B cell activation that are upregulated in macaque neonatal B cells are *CD79B,* which is critical for B cell receptor (BCR) signaling (Cassard et al., 1996; Costa et al., 1992; Hombach et al., 1990); *FCRL1* (Davis et al., 2001; Leu et al., 2005) and *CD40* (Elgueta et al., 2009; Grewal and Flavell, 1998), which are critical for T-cell-dependent B cell activation; and *MAP3K8,* a kinase critical for transducing the CD40 signal within B cells (Eliopoulos et al., 2003) (Figure 4C). Interestingly, neonatal B cells after vaccination also upregulated transcripts associated with naive/MZ B cells (*IGHM*, *CD1C*, *CD22*, and *BTLA*) (Demberg et al., 2015; Weller et al., 2004), consistent with previous reports of increased expression of IgM and CD1c on MZ B cells in early childhood (Scheeren et al., 2008; de Vries et al., 2000b; Weill et al., 2009; Weller et al., 2008) (Figure 4D). In addition to activating B cell markers, we identified inhibitors of B cell activation (*CD72*, *SH3BP5*, and *NCOR1*) (Adachi et al., 2000; Tanaka et al., 2016; Yamadori et al., 1999) upregulated in neonate versus adult B cells, suggesting induction of groups of neonatal B cell transcripts that can either activate or inhibit B cell responses (Figure 4E). CD20 and the chemokine receptor CXCR4 are critical for B cell trafficking and are molecular targets for cancer immunotherapies (Beider et al., 2013; Nie et al., 2004; Reinholdt et al., 2016; Tedder et al., 1988). Interestingly, in both neonatal and adult macaques, the expression of the CD20 transcript *MS4A1* and the *CXCR4* transcript were expressed with little overlap or co-expression within the same B cell (Figure 4F), suggesting possible interactions between CD20 and CXCR4 (Beider et al., 2013; Reinholdt et al., 2016).

Frequency of B Cell Subsets in Peripheral Blood of Immunized Neonatal and Adult Macaques

We next compared B cell subsets in neonatal and adult macaques immunized with CH505 SOSIPs in studies 2 and 3. PBMCs collected 2 weeks after the first, third, and sixth immunizations were analyzed by flow cytometry for B cell subpopulations. We used the tSNE dimensional reduction algorithm to visualize and analyze multiple B cell populations in two-dimensional plots (Figures 5 and S3; Chester and Maecker, 2015). We identified eight B cell subsets among $CD20^{+}CD3^{-}CD14^{-}CD16^{-}$ lymphocytes: naive, IgM^{+} memory, IgG^{+} memory, $IgM^{-}IgG^{-}$ memory, IgM^{+} plasmablasts, IgM^{-} plasmablasts, MZ-like, and a rare population of undefined B cells characterized by expression of Ki67, CD1c, CD27, and high levels of IgM (Figure 5, Query 1). Across all time points post-vaccination, neonatal macaques had higher frequencies of naive B cells (neonate versus adult $p = 0.007$) and lower frequencies of IgG^{+} memory B cells (neonate versus adult $p = 0.0005$) and $IgM^{-}IgG^{-}$ memory B cells (neonate versus adult, $p = 0.0002$) than adults, while frequencies of IgM^{+} memory B cells were comparable between neonates and adult macaques (neonate versus adult $p = 0.69$) (Figure 5). IgM^{+} and IgM^{-} plasmablast frequencies were higher in adults than in neonates across all time points (neonate versus adult $p = 0.027$ for IgM^{+} plasmablast; $p = 0.04$ for IgM^{-} plasmablast) (Figure 5). However, neonates showed a higher frequency of B cells expressing a MZ-like phenotype ($CD20^{+}IgM^{+}CD38^{+}CD1c^{+}CD27^{-}CD21^{+}IgG^{-}$) (neonate versus adult $p = 0.00009$) (Figure 5) as well as more "Query 1" ($Ki67^{+}CD1c^{+}CD27^{+}IgM^{2+}$) B cells (neonate versus adult $p = 0.0007$) across all time points (Figure 5). These statistical assessments for Figure 5 were conducted using nonparametric longitudinal data analysis (see STAR Methods).

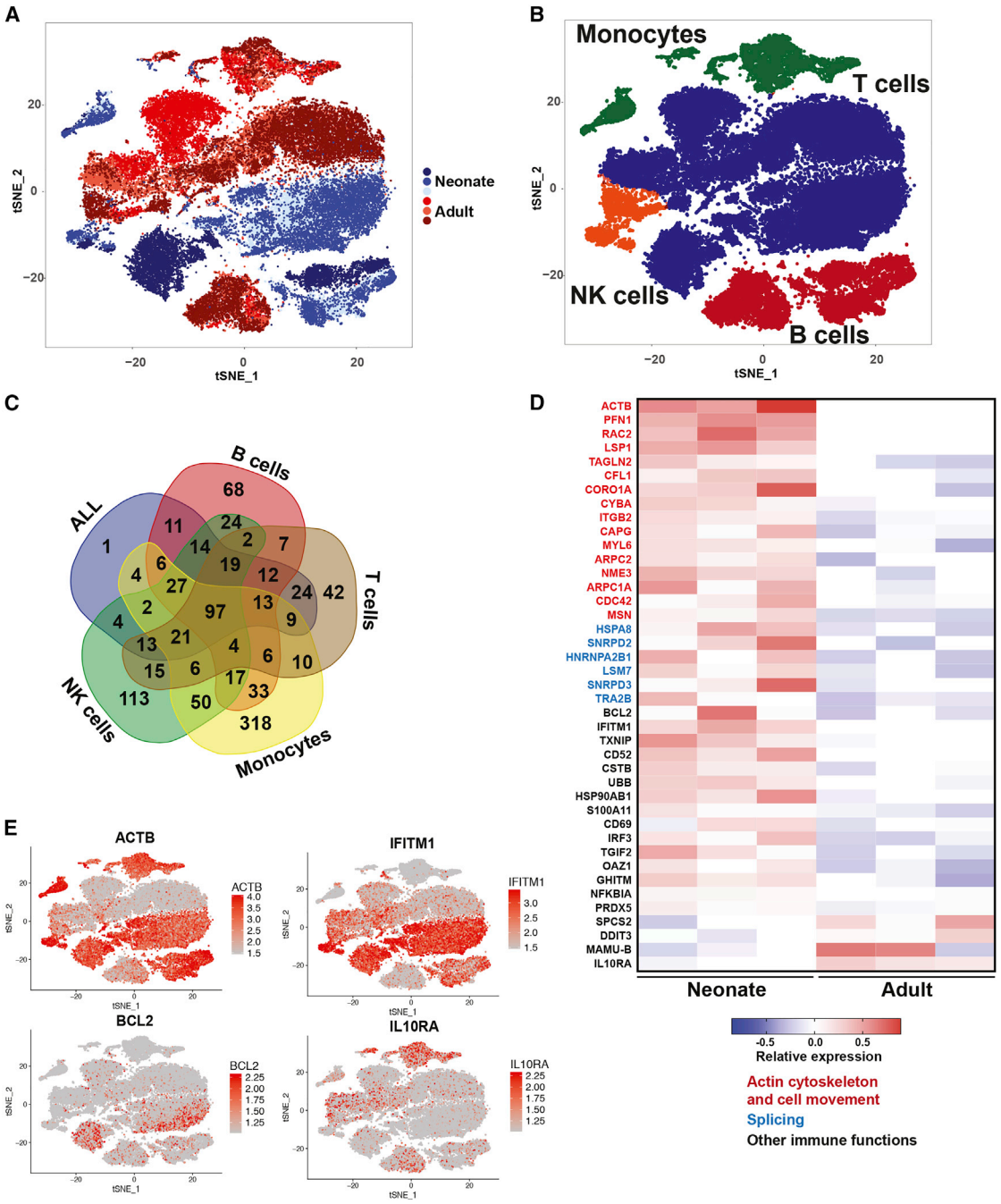

Figure 3. scRNA-Seq of PBMCs of HIV-1 Env-Immunized Neonatal and Adult Rhesus Macaques

(A) Two-dimensional plot from unsupervised clustering by t-distributed stochastic neighbor embedding (tSNE) of the single-cell transcriptomes from 52,306 PBMCs isolated from three neonate (blue) and three adult (red) rhesus macaques after CH505 SOSIPs immunization (week 9) in study 2.

(B) B, T, NK, and monocyte cells were identified within PBMCs on tSNE plot representation by expression of cell surface markers.

(C) Five-way Venn diagram of the differentially expressed genes (likelihood ratio test, $p \leq 0.05$) in neonate and adult cells detected in all four cell types combined (ALL), B cells, T cells, NK cells, and monocytes.

(D) Heatmap of representative transcripts that were changed in ALL populations. Panels represent individual macaques, and each pixel column is the expression of an individual cells. Transcripts are on the rows with the normalized expression (Z scores) colored by the legend (red, more upregulated; blue, more down-regulated). Genes with human orthologs are labeled and colored by known functional ontology (actin cytoskeleton and cell movement, red; RNA splicing, blue; other immune functions, black).

(E) Normalized ACTB, IFITM1, BCL2, and IL10RA transcript expression of single cells using tSNE plot representation.

See also Figure S2.

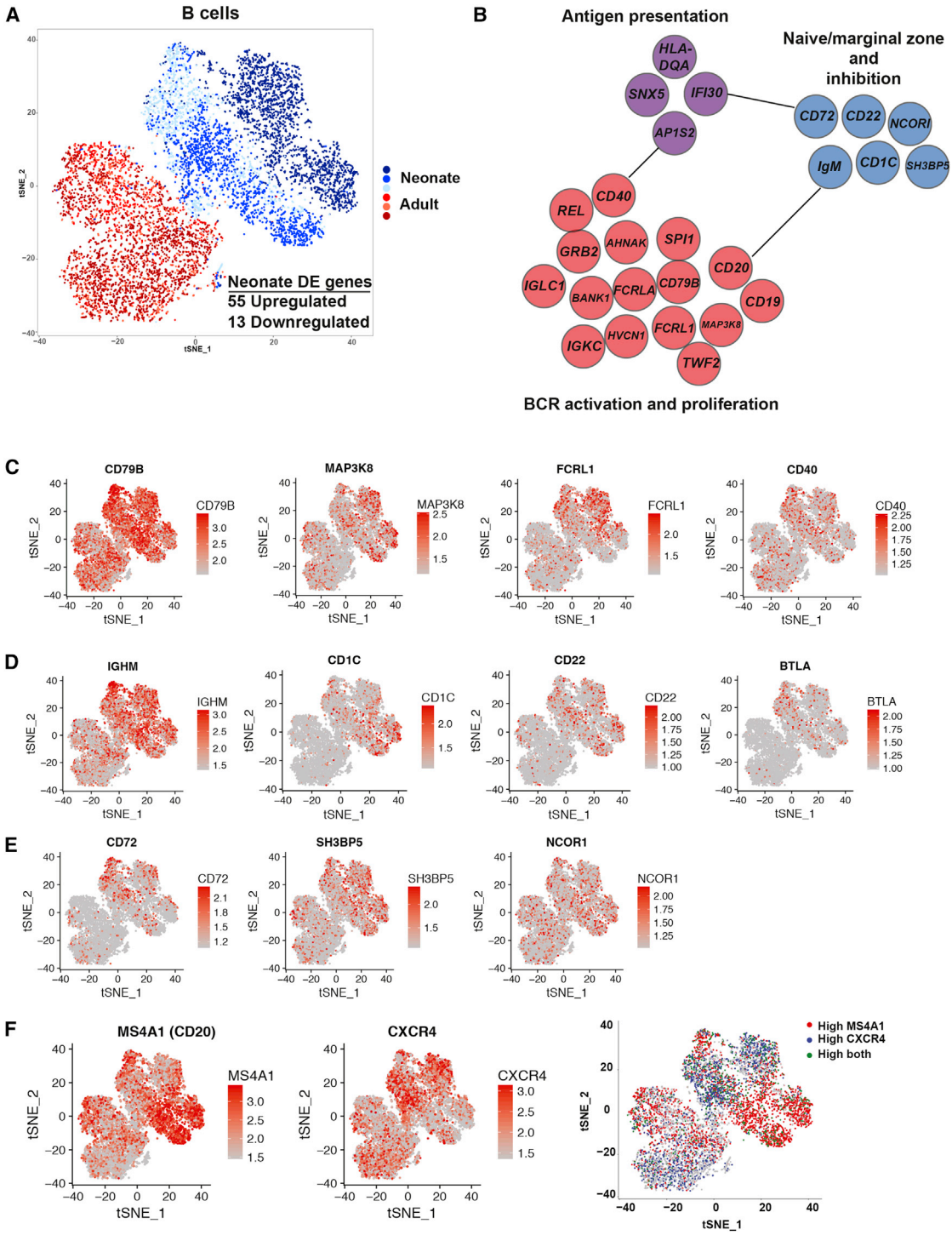

Figure 4. scRNA-Seq of B Cell Subsets of HIV-1 Env-Immunized Neonatal and Adult Rhesus Macaques

(A) Two-dimensional plot from unsupervised clustering by tSNE of the single-cell transcriptomes of the B cell cluster (MS4A1- and/or CD19-expressing cells) isolated from three neonate (blue) and three adult (red) rhesus macaques after the second immunization. 9,041 single cells are shown. The number of differentially expressed transcripts (likelihood ratio test, $p \leq 0.05$) upregulated or downregulated in neonatal B cells is shown.

(B) Transcripts upregulated in neonate B cells cluster in three functional groups (BCR activation and proliferation, red; antigen presentation, purple; naive/marginal zone and B cell inhibition, blue). Each circular node displays gene name.

(legend continued on next page)

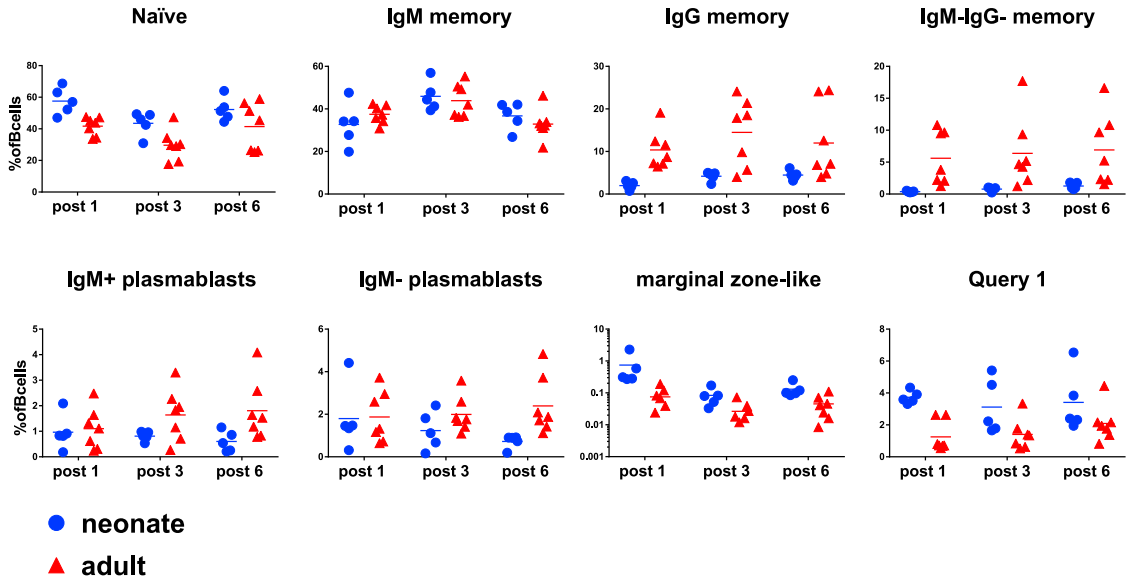

Figure 5. Frequency of B Cell Subsets in Peripheral Blood of HIV-1 Env-Immunized Neonatal and Adult Macaques

Frequency of eight B cell subsets, including naive, IgM^+ memory, IgG^+ memory, IgM^-IgG^- memory, IgM^+ plasmablasts, IgM^- plasmablasts, marginal zone-like (in log scale), and a rare population of undefined B cells (Query 1; $Ki67^+CD1c^+CD27^+$ IgM^{2+}) among $CD20^+CD3^-CD14^-CD16^-$ lymphocytes from CH505-SOSIP-immunized neonatal (blue) and adult (red) macaques in studies 2 and 3 measured by flow cytometry 2 weeks after the first, third, and sixth immunizations. Horizontal bars represent the group mean. nparLD was performed on SOSIP-immunized animals combined in studies 2 and 3 ($p = 0.007$ for naive, $p = 0.69$ for IgM^+ memory, $p = 0.0005$ for IgG^+ memory, $p = 0.0002$ for IgM^-IgG^- memory, $p = 0.027$ for IgM^+ plasmablasts, $p = 0.04$ for IgM^- plasmablasts, $p = 0.00009$ for marginal zone-like, and $p = 0.0007$ for Query 1). The scales of the y axis are different on each graph.

Increased Frequencies of Activated Blood Tfh Cells in Neonatal Macaques Compared to Adult Macaques

In addition to B cells, we studied T cell subsets in PBMCs by flow cytometry in studies 2 and 3 in animals immunized with SOSIP trimers (Figures 6 and S3). Across all time points, based on nonparametric longitudinal data analysis (see STAR Methods), neonatal macaques had higher frequency of total $CD4^+$ T cells (neonate versus adult $p = 0.017$) and naive $CD4^+$ T cells (neonate versus adult $p = 0.002$) but lower frequencies of $CD8^+$ T cells (neonate versus adult $p = 0.016$), effector memory $CD4^+$ T cells (neonate versus adult $p = 0.006$), and effector memory $CD8^+$ T cells (neonate versus adult $p = 0.005$) than adult macaques (Figure 6), consistent with the findings of different T lymphocyte subsets in human neonates and adults (Schatorjé et al., 2012; Shearer et al., 2003). The frequencies of naive $CD8^+$ T cells, central memory $CD4^+$ T cells, central memory $CD8^+$ T cells, and regulatory T (Treg) cells were not significantly different, which is also consistent with the findings in humans (Schatorjé et al., 2012). T follicular helper-like (Tfh) cells are required for the survival and selection of B cells within germinal centers in lymphoid tissues, and a circulating counterpart (circulating Tfh [cTfh] cells) has been implicated as an indicator of Tfh cell activity in tissues (Abbott et al., 2018; Locci et al., 2013). The frequency of $PD1^+CXCR5^+$ cTfh cells within $CD4^+$ T cells was not significantly different between neonatal and adult macaques across all time points (Figure 6). cTfh cells were further characterized by analyzing the Tfh cell markers inducible T cell costimulator (ICOS), Ki67, and CD69. The frequency of activated cTfh cells ($ICOS^{hi}Ki67^+$ or $ICOS^{hi}CD69^+$) within cTfh cells was increased across all time points in neonates compared with adults based on nonparametric longitudinal data analysis (neonate versus adult $p = 0.003$ for $ICOS^{hi}Ki67^+$; neonate versus adult $p = 0.002$ for $ICOS^{hi}CD69^+$) (Figure 6).

Transcriptional Differences in T Cells and Monocytes in Neonate and Adult Blood

Since we observed differences between the frequency of neonatal and adult macaque activated T cell subsets in the context of gp140 SOSIP immunization, we next studied the transcriptome of T cells in neonatal and adult macaques from study 2 after two immunizations (Figure S4A). T cells (*CD3D* expressing) of neonatal and adult macaques formed distinct clusters based on their cellular transcriptomes (Figure S4A). Unsupervised clustering identified 19 (T0–T18) distinct T cell transcriptional clusters (Figures S4A and S4B). 42 transcripts that were uniquely DE in neonatal and adult T cells were identified (Figure 3; Table S3). For example, neonatal T cells upregulated integrin, adhesion encoding transcripts (*ITGB7*, *ICAM3*, and *ITGA6*), and the transcription factor *LEF1* (Willinger et al., 2006) but had lower expression of the transcription factors *ETS1* and *AHI1* (Kaskow et al., 2018; Muthusamy et al., 1995; Figures S4C and S4D).

(C–E) Normalized transcript expression of single cells using tSNE plot representation. Examples of transcripts involved in (C) B cell activation, (D) marginal zone B cells, and (E) naive lymphocytes and inhibitory molecules.

(F) Normalized transcript expression of MS4A1 and CXCR4 on tSNE plot representation. Legends indicate normalized transcript values. Overlay plot on the right labels MS4A1-expressing cells in red, CXCR4-expressing cells in blue, and co-expressing cells in green.

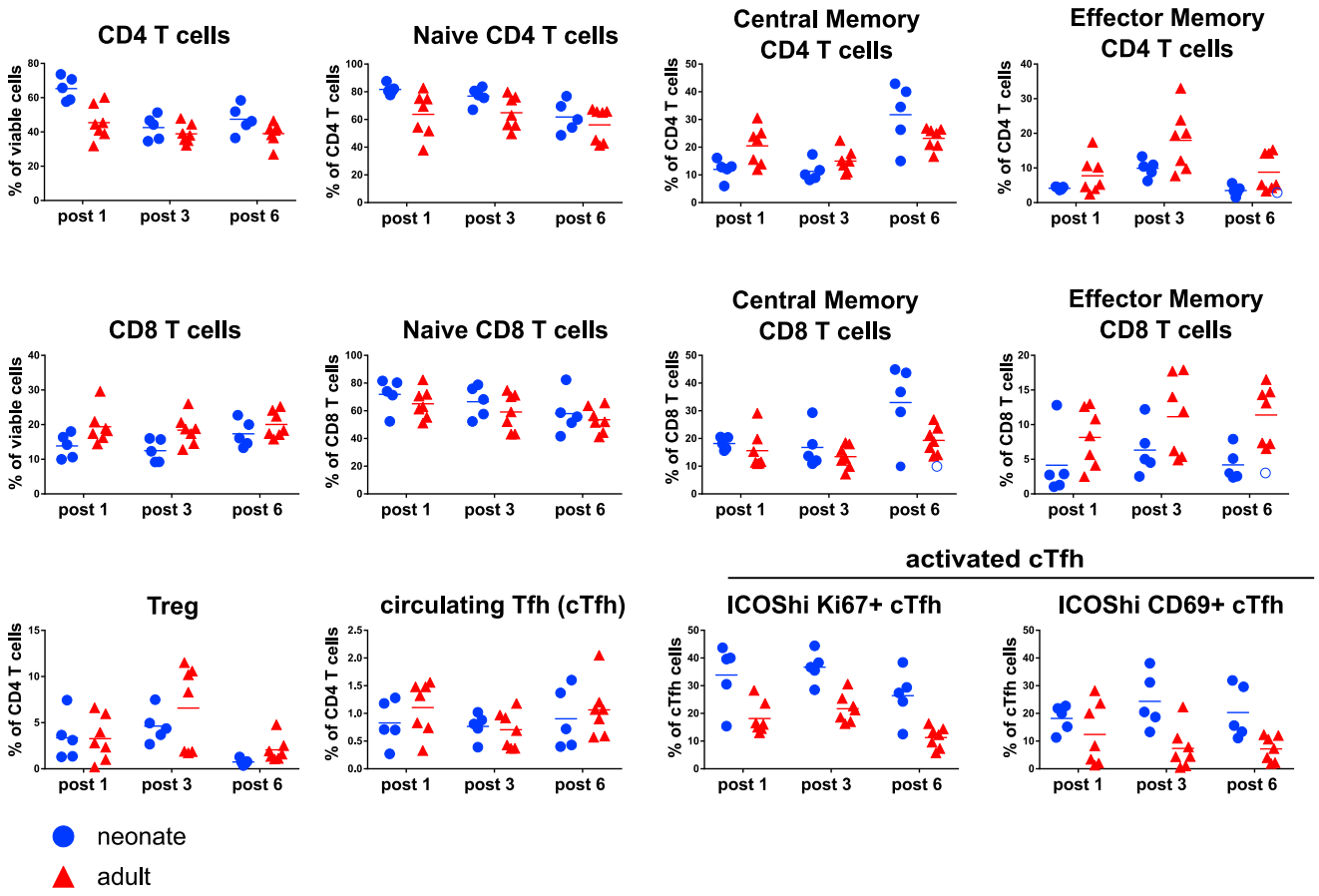

Figure 6. Increased Frequencies of Activated Blood T Follicular Helper-like (Tfh) Cells in Neonates Compared to Adults

The frequency of T cell subsets from CH505-SOSIP-immunized neonatal (blue) and adult (red) macaques in studies 2 and 3 measured by flow cytometry 2 weeks after the first, third, and sixth immunizations. $CD4^+$ T cells, $p = 0.017$; naive $CD4^+$ T cells, $p = 0.002$; central memory (CM) $CD4^+$ T cells, $p > 0.05$; effector memory (EM) $CD4^+$ T cells, $p = 0.006$; $CD8^+$ T cells, $p = 0.016$; naive $CD8^+$ T cells, $p > 0.05$; CM $CD8^+$ T cells, $p > 0.05$; EM $CD8^+$ T cells, $p = 0.005$; Treg cells, $p > 0.05$; circulating Tfh (cTfh) cells, $p > 0.05$; and activated cTfh cells ($ICOS^{hi}Ki67^+$, $p = 0.003$; $ICOS^{hi}$ $CD69^+$, $p = 0.002$). Horizontal bars are the group mean. nparLD was performed on SOSIP-immunized animals combined in studies 2 and 3.

Additionally, neonatal and adult blood monocytes (*CD14*, *LYZ* expressing) from study 2 clustered distinctly, but monocytes from individual neonatal and adult macaques also exhibited distinct transcriptomes, indicating high levels of individual transcriptional heterogeneity (Figure S5A). Unsupervised graph-based clustering identified seven distinct monocyte transcriptional clusters (M0–M6) (Figures S5A and S5B). Overall, we identified 318 transcripts that were DE in neonatal monocytes compared to adult monocytes (Figure 3; Table S5), such as RNAase (*RNASE6*), the RNA editor *APOBEC3A* (Becknell et al., 2015; Rosenberg and Dyer, 1996; Sharma et al., 2015), the innate inflammatory molecule allograft inflammatory factor-1 (*AIF1*), and the damage-associated membrane protein (DAMP) *S100A8* (Nacken et al., 2003; Ohsawa et al., 2000; Ryckman et al., 2003; Yang et al., 2005), that were upregulated in neonatal monocytes (Figures S5C and S5D).

To confirm differential transcriptome expression in neonatal and adult macaque immune cells, we performed scRNA-seq on 7,814 PBMCs from a neonatal macaque and 6,464 cells from an adult macaque in gp140 SOSIP immunization study 3 after the second immunization (week 6). We found that stabilized SOSIP-immunized neonatal and adult macaques had similar clustering patterns among all cell types as observed in single cells from macaques immunized with CH505 SOSIPs in study 2 (Figures S6A–S6C; Tables S7 and S8). Moreover, neonatal B cells had similar upregulation of transcripts associated with B cell activation (Figure S6D), naive and MZ-like B cells (Figure S6E), and B cell inhibitory molecules (Figure S6F), as observed in CH505-SOSIP-immunized neonates in study 2 (Figure 4). Thus, in two cohorts of neonates and adults immunized with SOSIP trimers, we found similar transcriptional program differences between neonatal and adult macaques.

Bacterial Composition of Fecal Microbiota in Neonatal and Adult Macaques

Since the gut microbiome can influence antibody responses to HIV-1 Env (Han et al., 2017; Williams et al., 2015, 2018), we wondered whether the gut microbiome could be one factor that shaped the neonatal and adult Env immune responses. Thus, we compared the microbiome of CH505-SOSIP-immunized

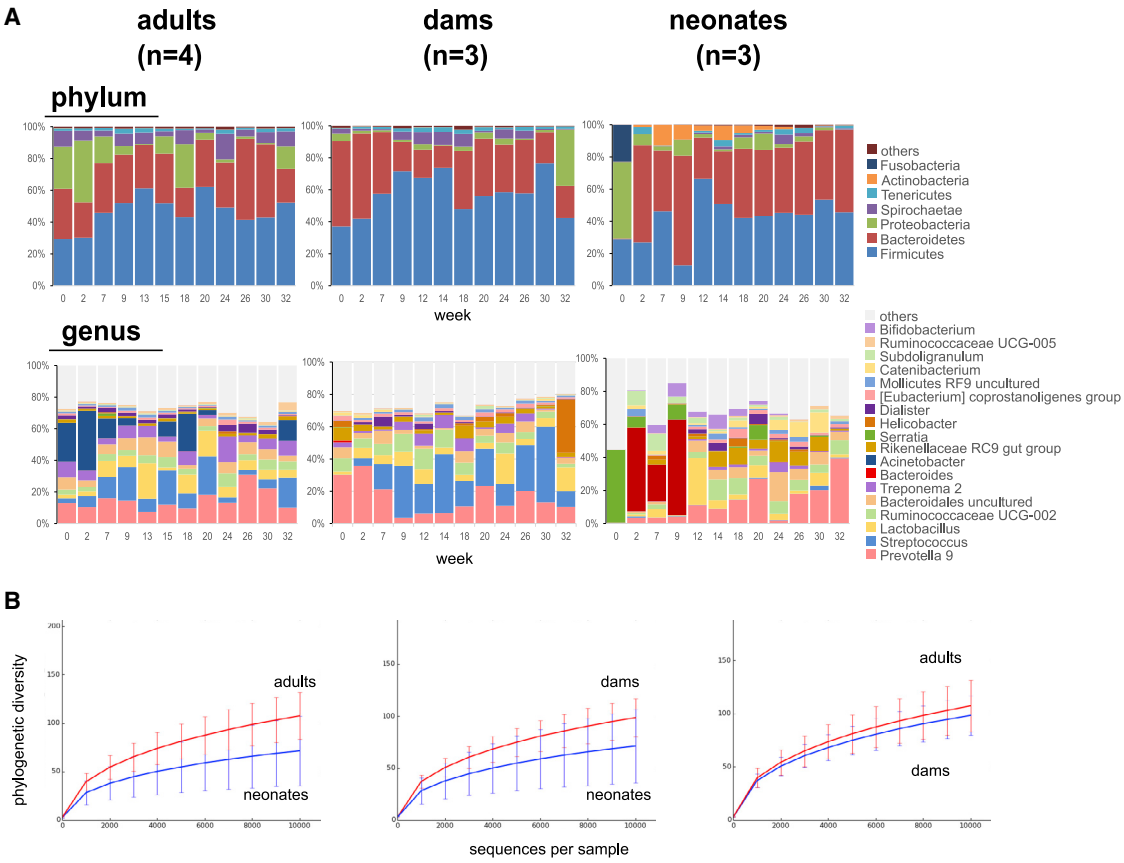

Figure 7. Compositions of Fecal Microbiota in Neonatal Rhesus Macaques, Unrelated Adult Rhesus Macaques, and Dams (Moms)

(A) The 16S rRNA amplicons of the stool samples from neonatal and adult rhesus macaques and dams were pyrosequenced and classified by comparison with the database at the phylum and genus levels. The relative proportions of the microbial taxa classified are plotted against time.

(B) Rarefaction curves plotted for phylogenetic distance as measures of alpha diversity.

neonatal macaques in study 2, dams (moms), and unrelated adult macaques by 16S ribosomal RNA (rRNA) analysis on fecal samples over time during vaccination. Colonization of the microbiome occurred early within the first week of life in neonatal macaques (Figure 7A). The most abundant phyla in the fecal samples of adult, dam, and neonatal macaques were Firmicutes and Bacteroidetes (Figure 7A), consistent with previous findings in macaques (Han et al., 2017; McKenna et al., 2008). On the genus level, the compositions of fecal microbiota in neonatal macaques were dynamic at early time points (<9 weeks) and became similar to adults and dams at later time points (Figure 7A). Rarefaction curves generated for the phylogenetic distance showed that the fecal microbiota of adult macaques and dams demonstrated greater diversity than those of neonatal macaques (Figure 7B). Thus, the composition of neonatal fecal microbiota was dynamic at early time points and underwent changes toward a composition similar to adult macaques. These data also raised the hypothesis that early development of the microbiome as soon as within 1 week of life may imprint neonatal B cell immunity to similarly respond to HIV-1 Envs like adults and are consistent with previous studies that suggested B cell imprinting by the microbiota soon after birth (Nguyen et al., 2016; Wesemann et al., 2013).

DISCUSSION

In this study, we have demonstrated that the neonatal immune system in rhesus macaques is capable of responding to HIV-1 Env gp120 monomer or SOSIP trimer immunogens and can generate levels of plasma Env-binding antibodies similar to adult macaques. Neonatal and adult macaques also elicited similar quality of plasma neutralizing antibodies and blood-derived B cell repertoires that responded to the HIV-1 Env immunogens. Neonatal macaques had a distinct transcriptome profile of increased *BCL2* in T cells and decreased *IL10RA* transcripts in T, B, and NK cells and monocytes of post-vaccination immune cells compared to adult macaques. Moreover, neonatal macaques had a higher frequency of activated cTfh T cells across all time points compared with adults.

The hepatitis B surface antigen vaccine induced higher antibody responses in human newborns than in adults (Ota et al., 2004), whereas the diphtheria, pertussis, and tetanus vaccine induced lower concentrations of antibodies in young infants (Siegrist, 2001). Here, we show that both CH505 sequential gp120 and gp140 SOSIP Envs elicited comparable antibody responses in neonatal and adult macaques.

Given the structural properties and poly-reactivity of some HIV-1 Env-reactive antibodies, including bnAbs (Haynes et al., 2005b; Mouquet et al., 2010), immune tolerance controls have been reported to limit the development of neutralizing antibodies (NAbs) (Haynes and Verkoczy, 2014; Kelsoe and Haynes, 2017). Recent reports indicate that babies can make HIV-1 Env bnAbs at a higher frequency than adults and do so faster than adults as observed within 1 year of infection (Goo et al., 2014; Muenchhoff et al., 2016), which may indicate a more permissive immune environment of the development of HIV-1 bnAbs. Single-cell transcriptomic analysis of neonatal versus adult blood immune cells showed elevated transcripts that encoded the apoptosis regulatory BCL2 (*BCL2)* in neonatal T cells and decreased *IL10RA* transcripts in neonatal T, B, and NK cells and monocytes, suggesting that the developing infant immune system may have less stringent immune controls of HIV-1 Env-reactive antibodies. While neonatal B cells have upregulation of transcripts associated with naive lymphocytes and inhibitory molecules, neonatal B cells also expressed higher levels of activation markers, suggesting a lower B cell activation threshold than adult B cells. Additional factors related to vaccination regimens may also be important for bnAb induction even in a more permissive immune system. It remains to be determined how the transcriptome of neonate immune cells changes due to HIV-1 Env vaccine regimens, because we were unable to obtain pre-vaccination samples for transcriptome analysis in neonates. We speculate that the transcriptome differences in post-vaccination immune cells in neonatal and adult macaques may be due to intrinsic differences in neonatal and adult immune systems, including the cell subsets that are capable of responding to HIV-1 Env vaccines. Previous studies have suggested that neonates may have specific immune cell subsets and features that are different than adults, but they contribute similarly to HIV-1 Env immunity (Adkins et al., 2004; Martinez et al., 2015). Here, we studied the transcriptome of total PBMCs in a small sample size. Thus, additional pre- and post-vaccination transcriptome studies of neonate and adult macaques may be more informative for defining immune cell subsets that directly impact humoral HIV-1 Env immunity.

While neonates have a transcriptional pattern suggestive of more hyperreactive B cells, immunization of neonates with either sequential gp120s or SOSIP trimers did not induce tier 2 autologous or heterologous neutralizing antibodies. It is not clear why no autologous neutralizing antibodies were seen in these studies, since stabilized CH505 transmitted/founder SOSIP trimers have induced tier 2 autologous NAbs in rabbits and sequential CH505 gp140s have induced autologous and heterologous neutralizing antibodies in select macaques (Saunders et al., 2017a). Adjuvants may impact neonatal immunity to vaccines (van Haren et al., 2016; Levy et al., 2013; Mastelic Gavillet et al., 2015). The TLR4 agonist GLA/SE or TLR3 agonist poly-ICLC (Alexopoulou et al., 2001; Behzad et al., 2012; Coler et al., 2010; Ma and Ross, 2005; Vono et al., 2018) elicited comparable antibody responses in neonates compared to adults in response to HIV-1 Env forms. Recently, it was discovered that TLR7/8 adjuvant improves the neonatal antibody response to pneumococcal vaccines (Dowling et al., 2017) and may improve HIV neutralizing antibody responses. In addition, our study suggests that the immunogens used for these studies are not optimized to promote the full maturation of bnAb B cell lineages, even in the setting of neonatal immunization. Thus, bnAbs were not induced, indicating the need for more specifically designed sequential Envs to overcome additional limitations on induction of bnAbs, including the development of Envs to select for improbable mutations that are common in bnAb B cell lineages (Williams et al., 2017; Bonsignori et al., 2017; Wiehe et al., 2018). Additionally, vaccine delivery platforms can impact neonatal immunity; replication-deficient viral vectors have been shown to elicit significantly higher antibody responses in human infants under 2 years compared with adults (Bliss et al., 2017), and the DNA measles vaccine induced significantly higher plaque reduction neutralization titers in neonatal mice compared with adults (Capozzo et al., 2006). In our studies, both DNA prime with protein boost and protein alone elicited comparable neonatal HIV-1 Env responses.

Neonatal B cells had higher gene expression levels of MZ-like B cell markers compared to adults, suggesting that this B cell pool may contribute to HIV-1 Env B cell immunity in neonates. HIV Env-specific B cells in adults and neonates exhibited IgG or IgM memory phenotype after the third and sixth immunizations. MZ-like B cells could be one of the precursors of these IgG or IgM memory B cells. This may be particularly important for HIV-1 vaccine development, since some broadly neutralizing anti-HIV-1 Env antibodies may be derived from MZ B cells that produce polyspecific autoantibodies and are subject to host tolerance control mechanisms (Bonsignori et al., 2014; Haynes et al., 2005a, 2005b).

Finally, the microbiome profiles in neonatal and adult macaques were studied, and we found that neonates were colonized soon after birth, indicating that microbial imprinting of the B cell repertoire (Wesemann et al., 2013) can occur within 1 week of birth. We previously showed that the intestinal microbiome influences vaccine-induced antibody responses (Han et al., 2017; Williams et al., 2015), but associations between specific microbial taxa and the quality of vaccine-induced antibody responses in neonates remains to be determined.

In summary, our studies suggest human neonates will be able to respond as well as adults to Env immunogens and may benefit from early immunization prior to sexual debut. Moreover, this study provides an initial insight into the transcriptome profile of neonate and adult macaques following HIV-1 vaccination. Future transcriptomic studies may expand on these approaches by studying specific immune cell subsets in a larger number of animals to define neonatal and adult immune cell subsets and their properties that may contribute to humoral responses to vaccines or pathogens.

STAR★METHODS

Detailed methods are provided in the online version of this paper and include the following:

- KEY RESOURCES TABLE
- LEAD CONTACT AND MATERIALS AVAILABILITY
- EXPERIMENTAL MODEL AND SUBJECT DETAILS
  - Vaccine Regimens and Study Groups
- METHOD DETAILS
  - Flow Cytometry Memory B Cell Sorting
  - Phenotypic Analysis by Flow Cytometry

- Ab Binding Specificities and Epitope Mapping
- Antibody-Dependent Cellular Phagocytosis Assay
- Plasma Binding to the Surface of HIV-1-Infected Cells
- Neutralization Assays
- PCR Isolation of Heavy and Light Chain Genes
- Transient and Recombinant Ab Expression
- Single-Cell RNA Sequencing of Rhesus Macaque PBMCs
- Microbiome Analysis

● QUANTIFICATION AND STATISTICAL ANALYSIS
● DATA AND CODE AVAILABILITY

SUPPLEMENTAL INFORMATION

Supplemental Information can be found online at https://doi.org/10.1016/j.celrep.2019.12.091.

ACKNOWLEDGMENTS

The authors thank Andres Salazar for providing poly-ICLC (Hiltonol, Oncovir); DeAnna Tenney, Derrick Goodman, Ashley Trama, Amanda Eaton, Justin Pollara, Dawn J. Marshall, Cindy Bowman, Andrew Foulger, Lawrence Armand, Guanhua Xie, Shi-Mao Xia, Melissa Cooper, Rachel Reed, Giovanna Hernandez, Esther Lee, Erika Dunford, Callie Vivian, Stormi Chadwick, Maggie Barr, Nelson Wu, and Sabrina Arora for technical assistance; Jennifer Watanabe, Colony Research Services of CNPRC, Deb Weiss, and John Misamore from Bioqual; the Center for HIV/AIDS Vaccine Immunology and Immunogen Discovery; the Duke GCB Sequencing and Genomic Technologies Core; and the Duke Human Vaccine Institute Viral Genetics and Analysis Core. CEM.NKR CCR5^{+} cells were obtained through the NIH AIDS Reagent Program, Division of AIDS, NIAID, NIH (Dr. Alexandra Trkola); and human soluble CD4 recombinant protein (sCD4) was obtained through the NIH AIDS Reagent Program, Division of AIDS, NIAID, NIH from Progenics. Research reported in this publication was supported by the NIH NIAID and the Center for HIV/AIDS Vaccine Immunology and Immunogen Discovery (CHAVI-ID, grant UM1-AI100645), Duke Consortia for HIV/AIDS Vaccine Development (CHAVD, grant AI031308), NIH NIAID extramural project grant R01AI140897 (W.B.W.), NIAID project grant R01-AI120801 (K.O.S.), the NIH NIAID Duke University Center for AIDS Research (CFAR; P30-AI-64518), the Office of Research Infrastructure Programs/OD (P51OD011107) (to CNPRC), and the intramural research program of the Vaccine Research Center, NIH, NIAID.

AUTHOR CONTRIBUTIONS

Q.H., T.B., and W.B.W. designed and performed experiments, analyzed data, and co-wrote the paper; T.B. performed single-cell RNA-seq and data analysis; Q.H. and D.W.C. performed cell subsets flow cytometry and data analysis; D.C.M. performed neutralization assays; K.J.W. performed computational analysis of antibody sequences; R.J.P., X.S., and Q.H. performed Ab binding assays; N.A.V., W.R., and Y.W. performed statistical analysis; R.W.E. and G.F. performed infected-cell-binding assays; O.M. performed 16S rRNA sequencing and analysis; S.R. and C.B.F. managed the vaccine formulation with GLA-SE and edited the paper; L.L.S. performed experiment immunizations, analyzed data, and edited the paper; K.K.A.V.R., M.G.L., and S.S. participated in experimental design and data analysis, managed the vaccination of the animals and sample collection, and edited the paper; G.D.T., K.O.S., S.R.P., and M.A.M. analyzed data, designed experiments, reviewed data, and edited the paper; and B.F.H. conceived and designed the study, reviewed all data, wrote the first draft of the paper, and co-wrote the paper.

DECLARATION OF INTERESTS

B.F.H. and K.O.S. have patent applications for some of the immunogens used in this study.

Received: May 28, 2019
Revised: October 16, 2019
Accepted: December 24, 2019
Published: February 4, 2020

REFERENCES

Abbott, R.K., Lee, J.H., Menis, S., Skog, P., Rossi, M., Ota, T., Kulp, D.W., Bhullar, D., Kalyuzhniy, O., Havenar-Daughton, C., et al. (2018). Precursor frequency and affinity determine B cell competitive fitness in germinal centers, tested with germline-targeting HIV vaccine immunogens. Immunity *48*, 133–146.e6.

Ackerman, M.E., Moldt, B., Wyatt, R.T., Dugast, A.S., McAndrew, E., Tsoukas, S., Jost, S., Berger, C.T., Sciaranghella, G., Liu, Q., et al. (2011). A robust, high-throughput assay to determine the phagocytic activity of clinical antibody samples. J. Immunol. Methods *366*, 8–19.

Adachi, T., Wakabayashi, C., Nakayama, T., Yakura, H., and Tsubata, T. (2000). CD72 negatively regulates signaling through the antigen receptor of B cells. J. Immunol. *164*, 1223–1229.

Adkins, B., Leclerc, C., and Marshall-Clarke, S. (2004). Neonatal adaptive immunity comes of age. Nat. Rev. Immunol. *4*, 553–564.

Alam, S.M., Aussedat, B., Vohra, Y., Meyerhoff, R.R., Cale, E.M., Walkowicz, W.E., Radakovich, N.A., Anasti, K., Armand, L., Parks, R., et al. (2017). Mimicry of an HIV broadly neutralizing antibody epitope with a synthetic glycopeptide. Sci. Transl. Med. *9*, eaai7521.

Alexopoulou, L., Holt, A.C., Medzhitov, R., and Flavell, R.A. (2001). Recognition of double-stranded RNA and activation of NF-kappaB by Toll-like receptor 3. Nature *413*, 732–738.

Ardeshir, A., Narayan, N.R., Méndez-Lagares, G., Lu, D., Rauch, M., Huang, Y., Van Rompay, K.K.A., Lynch, S.V., and Hartigan-O'Connor, D.J. (2014). Breast-fed and bottle-fed infant rhesus macaques develop distinct gut microbiotas and immune systems. Sci. Transl. Med. *6*, 252ra120.

Barouch, D.H., Stephenson, K.E., Borducchi, E.N., Smith, K., Stanley, K., McNally, A.G., Liu, J., Abbink, P., Maxfield, L.F., Seaman, M.S., et al. (2013). Protective efficacy of a global HIV-1 mosaic vaccine against heterologous SHIV challenges in rhesus monkeys. Cell *155*, 531–539.

Barouch, D.H., Tomaka, F.L., Wegmann, F., Stieh, D.J., Alter, G., Robb, M.L., Michael, N.L., Peter, L., Nkolola, J.P., Borducchi, E.N., et al. (2018). Evaluation of a mosaic HIV-1 vaccine in a multicentre, randomised, double-blind, placebo-controlled, phase 1/2a clinical trial (APPROACH) and in rhesus monkeys (NHP 13-19). Lancet *392*, 232–243.

Becknell, B., Eichler, T.E., Beceiro, S., Li, B., Easterling, R.S., Carpenter, A.R., James, C.L., McHugh, K.M., Hains, D.S., Partida-Sanchez, S., and Spencer, J.D. (2015). Ribonucleases 6 and 7 have antimicrobial function in the human and murine urinary tract. Kidney Int. *87*, 151–161.

Behzad, H., Huckriede, A.L.W., Haynes, L., Gentleman, B., Coyle, K., Wilschut, J.C., Kollmann, T.R., Reed, S.G., and McElhaney, J.E. (2012). GLA-SE, a synthetic toll-like receptor 4 agonist, enhances T-cell responses to influenza vaccine in older adults. J. Infect. Dis. *205*, 466–473.

Beider, K., Ribakovsky, E., Abraham, M., Wald, H., Weiss, L., Rosenberg, E., Galun, E., Avigdor, A., Eizenberg, O., Peled, A., and Nagler, A. (2013). Targeting the CD20 and CXCR4 pathways in non-hodgkin lymphoma with rituximab and high-affinity CXCR4 antagonist BKT140. Clin. Cancer Res. *19*, 3495–3507.

Binley, J.M., Wrin, T., Korber, B., Zwick, M.B., Wang, M., Chappey, C., Stiegler, G., Kunert, R., Zolla-Pazner, S., Katinger, H., et al. (2004). Comprehensive cross-clade neutralization analysis of a panel of anti-human immunodeficiency virus type 1 monoclonal antibodies. J Virol *78*, 13232–13252.

Bliss, C.M., Drammeh, A., Bowyer, G., Sanou, G.S., Jagne, Y.J., Ouedraogo, O., Edwards, N.J., Tarama, C., Ouedraogo, N., Ouedraogo, M., et al. (2017). Viral vector malaria vaccines induce high-level T cell and antibody responses in West African children and infants. Mol. Ther. *25*, 547–559.

Bonsignori, M., Wiehe, K., Grimm, S.K., Lynch, R., Yang, G., Kozink, D.M., Perrin, F., Cooper, A.J., Hwang, K.K., Chen, X., et al. (2014). An autoreactive antibody from an SLE/HIV-1 individual broadly neutralizes HIV-1. J. Clin. Invest. *124*, 1835–1843.

Bonsignori, M., Zhou, T., Sheng, Z., Chen, L., Gao, F., Joyce, M.G., Ozorowski, G., Chuang, G.Y., Schramm, C.A., Wiehe, K., et al.; NISC Comparative Sequencing Program (2016). Maturation pathway from germline to broad HIV-1 neutralizer of a CD4-mimic antibody. Cell *165*, 449–463.

Bonsignori, M., Kreider, E.F., Fera, D., Meyerhoff, R.R., Bradley, T., Wiehe, K., Alam, S.M., Aussedat, B., Walkowicz, W.E., Hwang, K.K., et al. (2017). Staged induction of HIV-1 glycan-dependent broadly neutralizing antibodies. Sci. Transl. Med. *9*, eaai7514.

Bradley, T., Pollara, J., Santra, S., Vandergrift, N., Pittala, S., Bailey-Kellogg, C., Shen, X., Parks, R., Goodman, D., Eaton, A., et al. (2017). Pentavalent HIV-1 vaccine protects against simian-human immunodeficiency virus challenge. Nat. Commun. *8*, 15711.

Bradley, T., Peppa, D., Pedroza-Pacheco, I., Li, D., Cain, D.W., Henao, R., Venkat, V., Hora, B., Chen, Y., Vandergrift, N.A., et al. (2018). RAB11FIP5 expression and altered natural killer cell function are associated with induction of HIV broadly neutralizing antibody responses. Cell *175*, 387–399.e17.

Brezinschek, H.P., Foster, S.J., Brezinschek, R.I., Dörner, T., Domiati-Saad, R., and Lipsky, P.E. (1997). Analysis of the human VH gene repertoire. Differential effects of selection and somatic hypermutation on human peripheral CD5(+)/IgM+ and CD5(-)/IgM+ B cells. J. Clin. Invest. *99*, 2488–2501.

Caporaso, J.G., Kuczynski, J., Stombaugh, J., Bittinger, K., Bushman, F.D., Costello, E.K., Fierer, N., Peña, A.G., Goodrich, J.K., Gordon, J.I., et al. (2010). QIIME allows analysis of high-throughput community sequencing data. Nat. Methods *7*, 335–336.

Capozzo, A.V., Ramírez, K., Polo, J.M., Ulmer, J., Barry, E.M., Levine, M.M., and Pasetti, M.F. (2006). Neonatal immunization with a Sindbis virus-DNA measles vaccine induces adult-like neutralizing antibodies and cell-mediated immunity in the presence of maternal antibodies. J. Immunol. *176*, 5671–5681.

Cassard, S., Choquet, D., Fridman, W.H., and Bonnerot, C. (1996). Regulation of ITAM signaling by specific sequences in Ig-beta B cell antigen receptor subunit. J. Biol. Chem. *271*, 23786–23791.

Chester, C., and Maecker, H.T. (2015). Algorithmic tools for mining high-dimensional cytometry data. J. Immunol. *195*, 773–779.

Coler, R.N., Baldwin, S.L., Shaverdian, N., Bertholet, S., Reed, S.J., Raman, V.S., Lu, X., DeVos, J., Hancock, K., Katz, J.M., et al. (2010). A synthetic adjuvant to enhance and expand immune responses to influenza vaccines. PLoS ONE *5*, e13677.

Costa, T.E., Franke, R.R., Sanchez, M., Misulovin, Z., and Nussenzweig, M.C. (1992). Functional reconstitution of an immunoglobulin antigen receptor in T cells. J. Exp. Med. *175*, 1669–1676.

Cunningham, C.K., Wara, D.W., Kang, M., Kang, M., Fenton, T., Hawkins, K., McNamara, J., Mofenson, L., Duliege, A.M., Francis, D., et al. (2001). Safety of two recombinant HIV-1 envelope vaccines in neonates born to HIV-1 infected women. Clin. Infect. Dis. *32*, 801–807.

Davis, R.S., Wang, Y.H., Kubagawa, H., and Cooper, M.D. (2001). Identification of a family of Fc receptor homologs with preferential B cell expression. Proc. Natl. Acad. Sci. USA *98*, 9772–9777.

de Taeye, S.W., Ozorowski, G., Torrents de la Peña, A., Guttman, M., Julien, J.P., van den Kerkhof, T.L.G.M., Burger, J.A., Pritchard, L.K., Pugach, P., Yasmeen, A., et al. (2015). Immunogenicity of Stabilized HIV-1 Envelope Trimers with Reduced Exposure of Non-neutralizing Epitopes. Cell *163*, 1702–1715.

de Vries, E., de Bruin-Versteeg, S., Comans-Bitter, W.M., de Groot, R., Hop, W.C.J., Boerma, G.J.M., Lotgering, F.K., and van Dongen, J.J.M. (2000a). Longitudinal survey of lymphocyte subpopulations in the first year of life. Pediatr. Res. *47*, 528–537.

de Vries, E., de Bruin-Versteeg, S., Comans-Bitter, W.M., de Groot, R., Hop, W.C.J., Boerma, G.J.M., Lotgering, F.K., Sauer, P.J.J., and van Dongen, J.J.M. (2000b). Neonatal blood lymphocyte subpopulations: a different perspective when using absolute counts. Biol. Neonate *77*, 230–235.

De Wit, D., Tonon, S., Olislagers, V., Goriely, S., Boutriaux, M., Goldman, M., and Willems, F. (2003). Impaired responses to toll-like receptor 4 and toll-like receptor 3 ligands in human cord blood. J. Autoimmun. *21*, 277–281.

Demberg, T., Mohanram, V., Musich, T., Brocca-Cofano, E., McKinnon, K.M., Venzon, D., and Robert-Guroff, M. (2015). Loss of marginal zone B-cells in SHIVSF162P4 challenged rhesus macaques despite control of viremia to low or undetectable levels in chronic infection. Virology *484*, 323–333.

Dobin, A., Davis, C.A., Schlesinger, F., Drenkow, J., Zaleski, C., Jha, S., Batut, P., Chaisson, M., and Gingeras, T.R. (2013). STAR: ultrafast universal RNA-seq aligner. Bioinformatics *29*, 15–21.

Doores, K.J., and Burton, D.R. (2010). Variable loop glycan dependency of the broad and potent HIV-1-neutralizing antibodies PG9 and PG16. J. Virol. *84*, 10510–10521.

Doria-Rose, N.A., Schramm, C.A., Gorman, J., Moore, P.L., Bhiman, J.N., DeKosky, B.J., Ernandes, M.J., Georgiev, I.S., Kim, H.J., Pancera, M., et al.; NISC Comparative Sequencing Program (2014). Developmental pathway for potent V1V2-directed HIV-neutralizing antibodies. Nature *509*, 55–62.

Dowling, D.J., van Haren, S.D., Scheid, A., Bergelson, I., Kim, D., Mancuso, C.J., Foppen, W., Ozonoff, A., Fresh, L., Theriot, T.B., et al. (2017). TLR7/8 adjuvant overcomes newborn hyporesponsiveness to pneumococcal conjugate vaccine at birth. JCI Insight *2*, e91020.

Elgueta, R., Benson, M.J., de Vries, V.C., Wasiuk, A., Guo, Y., and Noelle, R.J. (2009). Molecular mechanism and function of CD40/CD40L engagement in the immune system. Immunol. Rev. *229*, 152–172.

Eliopoulos, A.G., Wang, C.C., Dumitru, C.D., and Tsichlis, P.N. (2003). Tpl2 transduces CD40 and TNF signals that activate ERK and regulates IgE induction by CD40. EMBO J. *22*, 3855–3864.

Ferrari, G., Pollara, J., Kozink, D., Harms, T., Drinker, M., Freel, S., Moody, M.A., Alam, S.M., Tomaras, G.D., Ochsenbauer, C., et al. (2011). An HIV-1 gp120 envelope human monoclonal antibody that recognizes a C1 conformational epitope mediates potent antibody-dependent cellular cytotoxicity (ADCC) activity and defines a common ADCC epitope in human HIV-1 serum. J. Virol. *85*, 7029–7036.

Fouda, G.G., Cunningham, C.K., McFarland, E.J., Borkowsky, W., Muresan, P., Pollara, J., Song, L.Y., Liebl, B.E., Whitaker, K., Shen, X., et al. (2015). Infant HIV type 1 gp120 vaccination elicits robust and durable anti-V1V2 immunoglobulin G responses and only rare envelope-specific immunoglobulin A responses. J. Infect. Dis. *211*, 508–517.

Gans, H.A., Arvin, A.M., Galinus, J., Logan, L., DeHovitz, R., and Maldonado, Y. (1998). Deficiency of the humoral immune response to measles vaccine in infants immunized at age 6 months. JAMA *280*, 527–532.

Gao, F., Bonsignori, M., Liao, H.X., Kumar, A., Xia, S.M., Lu, X., Cai, F., Hwang, K.K., Song, H., Zhou, T., et al. (2014). Cooperation of B cell lineages in induction of HIV-1-broadly neutralizing antibodies. Cell *158*, 481–491.

Gao, F., Morrison, S.G., Robertson, D.L., Thornton, C.L., Craig, S., Karlsson, G., Sodroski, K., Morgado, M., Galvao-Castro, B., and von Briesen, H. (1996). Molecular cloning and analysis of functional envelope genes from human immunodeficiency virus type 1 sequence subtypes A through G. The WHO and NIAID Networks for HIV Isolation and Characterization. J Virol *70*, 1651–1667.

Garces, F., Sok, D., Kong, L., McBride, R., Kim, H.J., Saye-Francisco, K.F., Julien, J.P., Hua, Y., Cupo, A., Moore, J.P., et al. (2014). Structural evolution of glycan recognition by a family of potent HIV antibodies. Cell *159*, 69–79.

Gnanakaran, S., Daniels, M.G., Bhattacharya, Y., Lapedes, A.S., Sethi, A., Li, M., Tang, H., Greene, K., Gao, H., Haynes, B.F., et al. (2010). Genetic signatures in the envelope glycoproteins of HIV-1 that associate with broadly neutralizing antibodies. PLoS Comput Biol *6*, E1000955.

Goo, L., Chohan, V., Nduati, R., and Overbaugh, J. (2014). Early development of broadly neutralizing antibodies in HIV-1-infected infants. Nat. Med. *20*, 655–658.

Grewal, I.S., and Flavell, R.A. (1998). CD40 and CD154 in cell-mediated immunity. Annu. Rev. Immunol. *16*, 111–135.

Gruber, W.C., Darden, P.M., Still, J.G., Lohr, J., Reed, G., and Wright, P.F. (1997). Evaluation of bivalent live attenuated influenza A vaccines in children 2 months to 3 years of age: safety, immunogenicity and dose-response. Vaccine *15*, 1379–1384.

Han, Q., Williams, W.B., Saunders, K.O., Seaton, K.E., Wiehe, K.J., Vandergrift, N., Von Holle, T.A., Trama, A.M., Parks, R.J., Luo, K., et al. (2017). HIV DNA-

adenovirus multiclade envelope vaccine induces gp41 antibody immunodominance in rhesus macaques. J. Virol. *91*, e00923–e17.

Havenar-Daughton, C., Carnathan, D.G., Torrents de la Peña, A., Pauthner, M., Briney, B., Reiss, S.M., Wood, J.S., Kaushik, K., van Gils, M.J., Rosales, S.L., et al. (2016). Direct probing of germinal center responses reveals immunological features and bottlenecks for neutralizing antibody responses to HIV Env trimer. Cell Rep. *17*, 2195–2209.

Haynes, B.F., and Burton, D.R. (2017). Developing an HIV vaccine. Science *355*, 1129–1130.

Haynes, B.F., and Verkoczy, L. (2014). Host controls of HIV neutralizing antibodies. Science *344*, 588–589.

Haynes, B.F., Moody, M.A., Verkoczy, L., Kelsoe, G., and Alam, S.M. (2005a). Antibody polyspecificity and neutralization of HIV-1: a hypothesis. Hum. Antibodies *14*, 59–67.

Haynes, B.F., Fleming, J., St. Clair, E.W., Katinger, H., Stiegler, G., Kunert, R., Robinson, J., Scearce, R.M., Plonk, K., Staats, H.F., et al. (2005b). Cardiolipin polyspecific autoreactivity in two broadly neutralizing HIV-1 antibodies. Science *308*, 1906–1908.

Haynes, B.F., Gilbert, P.B., McElrath, M.J., Zolla-Pazner, S., Tomaras, G.D., Alam, S.M., Evans, D.T., Montefiori, D.C., Karnasuta, C., Sutthent, R., et al. (2012). Immune-correlates analysis of an HIV-1 vaccine efficacy trial. N. Engl. J. Med. *366*, 1275–1286.

Hombach, J., Tsubata, T., Leclercq, L., Stappert, H., and Reth, M. (1990). Molecular components of the B-cell antigen receptor complex of the IgM class. Nature *343*, 760–762.

Howell, D.N., Andreotti, P.E., Dawson, J.R., and Cresswell, P. (1985). Natural killing target antigens as inducers of interferon: studies with an immunoselected, natural killing-resistant human T lymphoblastoid cell line. J. Immunol. *134*, 971–976.

Hraber, P., Seaman, M.S., Bailer, R.T., Mascola, J.R., Montefiori, D.C., and Korber, B.T. (2014). Prevalence of broadly neutralizing antibody responses during chronic HIV-1 infection. AIDS *28*, 163–169.

Johnson, D.C., McFarland, E.J., Muresan, P., Fenton, T., McNamara, J., Read, J.S., Hawkins, E., Bouquin, P.L., Estep, S.G., Tomaras, G.D., et al. (2005). Safety and immunogenicity of an HIV-1 recombinant canarypox vaccine in newborns and infants of HIV-1-infected women. J. Infect. Dis. *192*, 2129–2133.

Kaskow, B.J., Buttrick, T.S., Klein, H.U., White, C., Bourgeois, J.R., Ferland, R.J., Patsopoulos, N., Bradshaw, E.M., De Jager, P.L., and Elyaman, W. (2018). MS AHI1 genetic risk promotes IFNγ+ CD4+ T cells. Neurol. Neuroimmunol. NeuroInflammation *5*, 1–10.

Kelsoe, G., and Haynes, B.F. (2017). Host controls of HIV broadly neutralizing antibody development. Immunol. Rev. *275*, 79–88.

Kepler, T.B. (2013). Reconstructing a B-cell clonal lineage. I. Statistical inference of unobserved ancestors. F1000Res. *2*, 103.

Kintu, K., Andrew, P., Musoke, P., Richardson, P., Asiimwe-Kateera, B., Nakyanzi, T., Wang, L., Fowler, M.G., Emel, L., Ou, S.S., et al. (2013). Feasibility and safety of ALVAC-HIV vCP1521 vaccine in HIV-exposed infants in Uganda: results from the first HIV vaccine trial in infants in Africa. J. Acquir. Immune Defic. Syndr. *63*, 1–8.

Kollmann, T.R., Kampmann, B., Mazmanian, S.K., Marchant, A., and Levy, O. (2017). Protecting the newborn and young infant from infectious diseases: lessons from immune ontogeny. Immunity *46*, 350–363.

Langrish, C.L., Buddle, J.C., Thrasher, A.J., and Goldblatt, D. (2002). Neonatal dendritic cells are intrinsically biased against Th-1 immune responses. Clin. Exp. Immunol. *128*, 118–123.

Lee, A.H., Shannon, C.P., Amenyogbe, N., Bennike, T.B., Diray-Arce, J., Idoko, O.T., Gill, E.E., Ben-Othman, R., Pomat, W.S., van Haren, S.D., et al.; EPIC Consortium (2019). Dynamic molecular changes during the first week of human life follow a robust developmental trajectory. Nat. Commun. *10*, 1092.

Leu, C.M., Davis, R.S., Gartland, L.A., Fine, W.D., and Cooper, M.D. (2005). FcRH1: an activation coreceptor on human B cells. Blood *105*, 1121–1126.

Levy, O., Goriely, S., and Kollmann, T.R. (2013). Immune response to vaccine adjuvants during the first year of life. Vaccine *31*, 2500–2505.

Liao, H.X., Levesque, M.C., Nagel, A., Dixon, A., Zhang, R., Walter, E., Parks, R., Whitesides, J., Marshall, D.J., Hwang, K.K., et al. (2009). High-throughput isolation of immunoglobulin genes from single human B cells and expression as monoclonal antibodies. J. Virol. Methods *158*, 171–179.

Li, Y., Gao, F., Mascola, J.R., Stamatatos, L., Polonis, V.R., Koutsoukos, M., Voss, G., Goepfert, P., Gilbert, P., Greene, K.M., et al. (2005). Human immunodeficiency virus type 1 env clones from acute and early subtype B infections for standardized assessments of vaccine-elicited neutralizing antibodies. J Virol *79*, 10108–10125.

Li, Y., Hui, H., Burgess, C.J., Price, R.W., Sharp, P.M., Hanh, B.H., and Shaw, B.M. (1992). Complete nucleotide sequence, genome organization, and biological properties of human immunodeficiency virus type 1 in vivo: evidence for limited defectiveness and complementation. J Virol *66*, 6587–6600.

Li, Y., Migueles, S.A., Welcher, B., Svehla, K., Phogat, A., Louder, M.K., Wu, X., Shaw, G.M., et al. (2007). Broad HIV-1 neutralization mediated by CD4-binding site antibodies. Nat Med *13*, 1032–1034.

Liao, H.X., Chen, X., Munshaw, S., Zhang, R., Marshall, D.J., Vandergrift, N., Whitesides, J.F., Lu, X., Yu, J.S., Hwang, K.K., et al. (2011). Initial antibodies binding to HIV-1 gp41 in acutely infected subjects are polyreactive and highly mutated. J. Exp. Med. *208*, 2237–2249.

Liao, H.X., Lynch, R., Zhou, T., Gao, F., Alam, S.M., Boyd, S.D., Fire, A.Z., Roskin, K.M., Schramm, C.A., Zhang, Z., et al.; NISC Comparative Sequencing Program (2013). Co-evolution of a broadly neutralizing HIV-1 antibody and founder virus. Nature *496*, 469–476.

Liao, H.X., Lynch, R., Zhou, T., Gao, F., Alam, S.M., Boyd, S.D., Fire, A.Z., Roskin, K.M., Schramm, C.A., Zhang, Z., et al. (2013). Co-evolution of a broadly neutralizing HIV-1 antibody and founder virus. Nature *496*, 469–476.

Locci, M., Havenar-Daughton, C., Landais, E., Wu, J., Kroenke, M.A., Arlehamn, C.L., Su, L.F., Cubas, R., Davis, M.M., Sette, A., et al.; International AIDS Vaccine Initiative Protocol C Principal Investigators (2013). Human circulating PD-1+CXCR3-CXCR5+ memory Tfh cells are highly functional and correlate with broadly neutralizing HIV antibody responses. Immunity *39*, 758–769.

Long, E.M., Rainwater, S.M., Lavreys, L., Mandaliya, K., and Overbaugh, J. (2002). HIV type 1 variants transmitted to women in Kenya require the CCR5 coreceptor for entry, regardless of the genetic complexity of the infecting virus. AIDS Res Hum Retroviruses *18*, 567–576.

Lyerly, H.K., Reed, D.L., Matthews, T.J., Langlois, A.J., Ahearne, P.A., Petteway, S.R., Jr., and Weinhold, K.J. (1987). Anti-GP 120 antibodies from HIV seropositive individuals mediate broadly reactive anti-HIV ADCC. AIDS Res. Hum. Retroviruses *3*, 409–422.

Ma, Y., and Ross, A.C. (2005). The anti-tetanus immune response of neonatal mice is augmented by retinoic acid combined with polyriboinosinic:polyribocytidylic acid. Proc. Natl. Acad. Sci. USA *102*, 13556–13561.

Mackenzie, L.E., Youinou, P.Y., Hicks, R., Yuksel, B., Mageed, R.A., and Lydyard, P.M. (1991). Auto- and polyreactivity of IgM from CD5+ and CD5- cord blood B cells. Scand. J. Immunol. *33*, 329–335.

Martinez, D.R., Permar, S.R., and Fouda, G.G. (2015). Contrasting adult and infant immune responses to HIV infection and vaccination. Clin. Vaccine Immunol. *23*, 84–94.

Mastelic Gavillet, B., Eberhardt, C.S., Auderset, F., Castellino, F., Seubert, A., Tregoning, J.S., Lambert, P.H., de Gregorio, E., Del Giudice, G., and Siegrist, C.A. (2015). MF59 mediates its B cell adjuvanticity by promoting T follicular helper cells and thus germinal center responses in adult and early life. J. Immunol. *194*, 4836–4845.

McDavid, A., Finak, G., Chattopadyay, P.K., Dominguez, M., Lamoreaux, L., Ma, S.S., Roederer, M., and Gottardo, R. (2013). Data exploration, quality control and testing in single-cell qPCR-based gene expression experiments. Bioinformatics *29*, 461–467.

McFarland, E.J., Borkowsky, W., Fenton, T., Wara, D., McNamara, J., Samson, P., Kang, M., Mofenson, L., Cunningham, C., Duliege, A.M., et al.; AIDS Clinical Trials Group 230 Collaborators (2001). Human immunodeficiency virus type 1 (HIV-1) gp120-specific antibodies in neonates receiving an HIV-1 recombinant gp120 vaccine. J. Infect. Dis. *184*, 1331–1335.

McFarland, E.J., Johnson, D.C., Muresan, P., Fenton, T., Tomaras, G.D., McNamara, J., Read, J.S., Douglas, S.D., Deville, J., Gurwith, M., et al. (2006). HIV-1 vaccine induced immune responses in newborns of HIV-1 infected mothers. AIDS *20*, 1481–1489.

McGuire, E.P., Fong, Y., Toote, C., Cunningham, C.K., McFarland, E.J., Borkowsky, W., Barnett, S., Itell, H.L., Kumar, A., Gray, G., et al. (2017). HIV-exposed infants vaccinated with an MF59/recombinant gp120 vaccine have higher-magnitude anti-V1V2 IgG responses than adults immunized with the same vaccine. J. Virol. *92*, e01070–e17.

McKenna, P., Hoffmann, C., Minkah, N., Aye, P.P., Lackner, A., Liu, Z., Lozupone, C.A., Hamady, M., Knight, R., and Bushman, F.D. (2008). The macaque gut microbiome in health, lentiviral infection, and chronic enterocolitis. PLoS Pathog. *4*, e20.

Melvan, J.N., Bagby, G.J., Welsh, D.A., Nelson, S., and Zhang, P. (2010). Neonatal sepsis and neutrophil insufficiencies. Int. Rev. Immunol. *29*, 315–348.

Mouquet, H., Scheid, J.F., Zoller, M.J., Krogsgaard, M., Ott, R.G., Shukair, S., Artyomov, M.N., Pietzsch, J., Connors, M., Pereyra, F., et al. (2010). Polyreactivity increases the apparent affinity of anti-HIV antibodies by heteroligation. Nature *467*, 591–595.

Muenchhoff, M., Adland, E., Karimanzira, O., Crowther, C., Pace, M., Csala, A., Leitman, E., Moonsamy, A., McGregor, C., Hurst, J., et al. (2016). Nonprogressing HIV-infected children share fundamental immunological features of nonpathogenic SIV infection. Sci. Transl. Med. *8*, 358ra125.

Muthusamy, N., Barton, K., and Leiden, J.M. (1995). Defective activation and survival of T cells lacking the Ets-1 transcription factor. Nature *377*, 639–642.

Nacken, W., Roth, J., Sorg, C., and Kerkhoff, C. (2003). S100A9/S100A8: myeloid representatives of the S100 protein family as prominent players in innate immunity. Microsc. Res. Tech. *60*, 569–580.

Narayan, N.R., Méndez-Lagares, G., Ardeshir, A., Lu, D., Van Rompay, K.K.A., and Hartigan-O'Connor, D.J. (2015). Persistent effects of early infant diet and associated microbiota on the juvenile immune system. Gut Microbes *6*, 284–289.

Neu, J. (2016). The microbiome during pregnancy and early postnatal life. Semin. Fetal Neonatal Med. *21*, 373–379.

Nguyen, Q.N., Himes, J.E., Martinez, D.R., and Permar, S.R. (2016). The impact of the gut microbiota on humoral immunity to pathogens and vaccination in early infancy. PLoS Pathog. *12*, e1005997.

Nie, Y., Waite, J., Brewer, F., Sunshine, M.J., Littman, D.R., and Zou, Y.R. (2004). The role of CXCR4 in maintaining peripheral B cell compartments and humoral immunity. J. Exp. Med. *200*, 1145–1156.

Noguchi, K., Gel, Y.R., Brunner, E., and Konietschke, F. (2012). nparLD: an R software package for the nonparametric analysis of longitudinal data. J. Stat. Softw. *50*, 1–23.

Ohsawa, K., Imai, Y., Kanazawa, H., Sasaki, Y., and Kohsaka, S. (2000). Involvement of Iba1 in membrane ruffling and phagocytosis of macrophages/microglia. J. Cell Sci. *113*, 3073–3084.

Ota, M.O.C., Vekemans, J., Schlegel-Haueter, S.E., Fielding, K., Whittle, H., Lambert, P.H., McAdam, K.P.W.J., Siegrist, C.A., and Marchant, A. (2004). Hepatitis B immunisation induces higher antibody and memory Th2 responses in new-borns than in adults. Vaccine *22*, 511–519.

Pauthner, M., Havenar-Daughton, C., Sok, D., Nkolola, J.P., Bastidas, R., Boopathy, A.V., Carnathan, D.G., Chandrashekar, A., Cirelli, K.M., Cottrell, C.A., et al. (2017). Elicitation of robust tier 2 neutralizing antibody responses in nonhuman primates by HIV envelope trimer immunization using optimized approaches. Immunity *46*, 1073–1088.e6.

Pejchal, R., Doores, K.J., Walker, L.M., Khayat, R., Huang, P.S., Wang, S.K., Stanfield, R.L., Julien, J.P., Ramos, A., Crispin, M., et al. (2011). A potent and broad neutralizing antibody recognizes and penetrates the HIV glycan shield. Science *334*, 1097–1103.

Phillips, B., Fouda, G.G., Eudailey, J., Pollara, J., Curtis, A.D., 2nd, Kunz, E., Dennis, M., Shen, X., Bay, C., Hudgens, M., et al. (2017). Impact of poxvirus vector priming, protein coadministration, and vaccine intervals on HIV gp120 vaccine-elicited antibody magnitude and function in infant macaques. Clin. Vaccine Immunol. *24*, e00231–e17.

Plebani, A., Proserpio, A.R., Guarneri, D., Buscaglia, M., and Cattoretti, G. (1993). B and T lymphocyte subsets in fetal and cord blood: age-related modulation of CD1c expression. Biol. Neonate *63*, 1–7.

PrabhuDas, M., Adkins, B., Gans, H., King, C., Levy, O., Ramilo, O., and Siegrist, C.A. (2011). Challenges in infant immunity: implications for responses to infection and vaccines. Nat. Immunol. *12*, 189–194.

Quast, C., Pruesse, E., Yilmaz, P., Gerken, J., Schweer, T., Yarza, P., Peplies, J., and Glöckner, F.O. (2013). The SILVA ribosomal RNA gene database project: improved data processing and web-based tools. Nucleic Acids Res. *41*, D590–D596.

Reinholdt, L., Laursen, M.B., Schmitz, A., Bødker, J.S., Jakobsen, L.H., Bøgsted, M., Johnsen, H.E., and Dybkær, K. (2016). The CXCR4 antagonist plerixafor enhances the effect of rituximab in diffuse large B-cell lymphoma cell lines. Biomark. Res. *4*, 12.

Rognes, T., Flouri, T., Nichols, B., Quince, C., and Mahé, F. (2016). VSEARCH: a versatile open source tool for metagenomics. PeerJ *4*, e2584.

Rosenberg, H.F., and Dyer, K.D. (1996). Molecular cloning and characterization of a novel human ribonuclease (RNase k6): increasing diversity in the enlarging ribonuclease gene family. Nucleic Acids Res. *24*, 3507–3513.

Ryckman, C., Vandal, K., Rouleau, P., Talbot, M., and Tessier, P.A. (2003). Proinflammatory activities of S100: proteins S100A8, S100A9, and S100A8/A9 induce neutrophil chemotaxis and adhesion. J. Immunol. *170*, 3233–3242.

Sanders, R.W., Derking, R., Cupo, A., Julien, J.P., Yasmeen, A., de Val, N., Kim, H.J., Blattner, C., de la Peña, A.T., Korzun, J., et al. (2013). A next-generation cleaved, soluble HIV-1 Env trimer, BG505 SOSIP.664 gp140, expresses multiple epitopes for broadly neutralizing but not non-neutralizing antibodies. PLoS Pathog. *9*, e1003618.

Sarzotti-Kelsoe, M., Bailer, R.T., Turk, E., Lin, C.L., Bilska, M., Greene, K.M., Gao, H., Todd, C.A., Ozaki, D.A., Seaman, M.S., et al. (2014). Optimization and validation of the TZM-bl assay for standardized assessments of neutralizing antibodies against HIV-1. J. Immunol. Methods *409*, 131–146.

Satija, R., Farrell, J.A., Gennert, D., Schier, A.F., and Regev, A. (2015). Spatial reconstruction of single-cell gene expression data. Nat. Biotechnol. *33*, 495–502.

Saunders, K.O., Verkoczy, L.K., Jiang, C., Zhang, J., Parks, R., Chen, H., Housman, M., Bouton-Verville, H., Shen, X., Trama, A.M., et al. (2017a). Vaccine induction of heterologous tier 2 HIV-1 neutralizing antibodies in animal models. Cell Rep. *21*, 3681–3690.

Saunders, K.O., Nicely, N.I., Wiehe, K., Bonsignori, M., Meyerhoff, R.R., Parks, R., Walkowicz, W.E., Aussedat, B., Wu, N.R., Cai, F., et al. (2017b). Vaccine elicitation of high mannose-dependent neutralizing antibodies against the V3-glycan broadly neutralizing epitope in nonhuman primates. Cell Rep. *18*, 2175–2188.

Scanlan, C.N., Ritchie, G.E., Baruah, K., Crispin, M., Harvey, D.J., Singer, B.B., Lucka, L., Wormald, M.R., Wentworth, P., Jr., Zitzmann, N., et al. (2007). Inhibition of mammalian glycan biosynthesis produces non-self antigens for a broadly neutralising, HIV-1 specific antibody. J. Mol. Biol. *372*, 16–22.

Schatorjé, E.J.H., Gemen, E.F.A., Driessen, G.J.A., Leuvenink, J., van Hout, R.W.N.M., and de Vries, E. (2012). Paediatric reference values for the peripheral T cell compartment. Scand. J. Immunol. *75*, 436–444.

Scheeren, F.A., Nagasawa, M., Weijer, K., Cupedo, T., Kirberg, J., Legrand, N., and Spits, H. (2008). T cell-independent development and induction of somatic hypermutation in human IgM^+ IgD^+ $CD27^+$ B cells. J. Exp. Med. *205*, 2033–2042.

Segata, N., Izard, J., Waldron, L., Gevers, D., Miropolsky, L., Garrett, W.S., and Huttenhower, C. (2011). Metagenomic biomarker discovery and explanation. Genome Biol. *12*, R60.

Seydoux, E., Liang, H., Dubois Cauwelaert, N., Archer, M., Rintala, N.D., Kramer, R., Carter, D., Fox, C.B., and Orr, M.T. (2018). Effective Combination Adjuvants Engage Both TLR and Inflammasome Pathways To Promote Potent Adaptive Immune Responses. J Immunol *201*, 98–112.

Sharma, S., Patnaik, S.K., Taggart, R.T., Kannisto, E.D., Enriquez, S.M., Gollnick, P., and Baysal, B.E. (2015). APOBEC3A cytidine deaminase induces RNA editing in monocytes and macrophages. Nat. Commun. *6*, 6881.

Shearer, W.T., Rosenblatt, H.M., Gelman, R.S., Oyomopito, R., Plaeger, S., Stiehm, E.R., Wara, D.W., Douglas, S.D., Luzuriaga, K., McFarland, E.J., et al.; Pediatric AIDS Clinical Trials Group (2003). Lymphocyte subsets in healthy children from birth through 18 years of age: the Pediatric AIDS Clinical Trials Group P1009 study. J. Allergy Clin. Immunol. *112*, 973–980.

Shen, X., Duffy, R., Howington, R., Cope, A., Sadagopal, S., Park, H., Pal, R., Kwa, S., Ding, S., Yang, O.O., et al. (2015). Vaccine-induced linear epitope-specific antibodies to simian immunodeficiency virus SIVmac239 envelope are distinct from those induced to the human immunodeficiency virus type 1 envelope in nonhuman primates. J. Virol. *89*, 8643–8650.

Siegrist, C.A. (2001). Neonatal and early life vaccinology. Vaccine *19*, 3331–3346.

Siegrist, C.A., and Aspinall, R. (2009). B-cell responses to vaccination at the extremes of age. Nat. Rev. Immunol. *9*, 185–194.

Simonich, C.A.A., Williams, K.L.L., Verkerke, H.P.P., Williams, J.A.A., Nduati, R., Lee, K.K.K., and Overbaugh, J. (2016). HIV-1 neutralizing antibodies with limited hypermutation from an infant. Cell *166*, 77–87.

Sok, D., Doores, K.J., Briney, B., Le, K.M., Saye-Francisco, K.L., Ramos, A., Kulp, D.W., Julien, J.P., Menis, S., Wickramasinghe, L., et al. (2014). Promiscuous glycan site recognition by antibodies to the high-mannose patch of gp120 broadens neutralization of HIV. Sci. Transl. Med. *6*, 236ra63.

Tanaka, H., Muto, A., Shima, H., Katoh, Y., Sax, N., Tajima, S., Brydun, A., Ikura, T., Yoshizawa, N., Masai, H., et al. (2016). Epigenetic regulation of the Blimp-1 gene (Prdm1) in B cells involves Bach2 and histone deacetylase 3. J. Biol. Chem. *291*, 6316–6330.

Tay, M.Z., Liu, P., Williams, L.D., McRaven, M.D., Sawant, S., Gurley, T.C., Xu, T.T., Dennison, S.M., Liao, H.X., Chenine, A.L., et al. (2016). Antibody-mediated internalization of infectious HIV-1 virions differs among antibody isotypes and subclasses. PLoS Pathog. *12*, e1005817.

Tedder, T.F., Streuli, M., Schlossman, S.F., and Saito, H. (1988). Isolation and structure of a cDNA encoding the B1 (CD20) cell-surface antigen of human B lymphocytes (lymphocyte differentiation antigen/gene expression/in vitro translation). Immunology *85*, 208–212.

Tomaras, G.D., and Plotkin, S.A. (2017). Complex immune correlates of protection in HIV-1 vaccine efficacy trials. Immunol. Rev. *275*, 245–261.

Tomaras, G.D., Yates, N.L., Liu, P., Qin, L., Fouda, G.G., Chavez, L.L., Decamp, A.C., Parks, R.J., Ashley, V.C., Lucas, J.T., et al. (2008). Initial B-cell responses to transmitted human immunodeficiency virus type 1: virion-binding immunoglobulin M (IgM) and IgG antibodies followed by plasma anti-gp41 antibodies with ineffective control of initial viremia. J. Virol. *82*, 12449–12463.

Tomaras, G.D., Binley, J.M., Gray, E.S., Crooks, E.T., Osawa, K., Moore, P.L., Tumba, N., Tong, T., Shen, X., Yates, N.L., et al. (2011). Polyclonal B cell responses to conserved neutralization epitopes in a subset of HIV-1-infected individuals. J. Virol. *85*, 11502–11519.

Trkola, A., Matthews, J., Gordon, C., Ketas, T., and Moore, J.P. (1999). A cell line-based neutralization assay for primary human immunodeficiency virus type 1 isolates that use either the CCR5 or the CXCR4 coreceptor. J. Virol. *73*, 8966–8974.

van Haren, S.D., Dowling, D.J., Foppen, W., Christensen, D., Andersen, P., Reed, S.G., Hershberg, R.M., Baden, L.R., and Levy, O. (2016). Age-specific adjuvant synergy: dual TLR7/8 and mincle activation of human newborn dendritic cells enables Th1 polarization. J. Immunol. *197*, 4413–4424.

Vekemans, J., Amedei, A., Ota, M.O., D'Elios, M.M., Goetghebuer, T., Ismaili, J., Newport, M.J., Del Prete, G., Goldman, M., McAdam, K.P., and Marchant, A. (2001). Neonatal bacillus Calmette-Guérin vaccination induces adult-like IFN-gamma production by CD4+ T lymphocytes. Eur. J. Immunol. *31*, 1531–1535.

Vono, M., Eberhardt, C.S., Mohr, E., Auderset, F., Christensen, D., Schmolke, M., Coler, R., Meinke, A., Andersen, P., Lambert, P.H., et al. (2018). Overcoming the neonatal limitations of inducing germinal centers through liposome-based adjuvants including C-type lectin agonists trehalose dibehenate or Curdlan. Front. Immunol. *9*, 381.

Weill, J.C., Weller, S., and Reynaud, C.A. (2009). Human marginal zone B cells. Annu. Rev. Immunol. *27*, 267–285.

Weller, S., Braun, M.C., Tan, B.K., Rosenwald, A., Cordier, C., Conley, M.E., Plebani, A., Kumararatne, D.S., Bonnet, D., Tournilhac, O., et al. (2004). Human blood IgM "memory" B cells are circulating splenic marginal zone B cells harboring a prediversified immunoglobulin repertoire. Blood *104*, 3647–3654.

Weller, S., Mamani-Matsuda, M., Picard, C., Cordier, C., Lecoeuche, D., Gauthier, F., Weill, J.C., and Reynaud, C.A. (2008). Somatic diversification in the absence of antigen-driven responses is the hallmark of the IgM^+ IgD^+ $CD27^+$ B cell repertoire in infants. J. Exp. Med. *205*, 1331–1342.

Wesemann, D.R., Portuguese, A.J., Meyers, R.M., Gallagher, M.P., Cluff-Jones, K., Magee, J.M., Panchakshari, R.A., Rodig, S.J., Kepler, T.B., and Alt, F.W. (2013). Microbial colonization influences early B-lineage development in the gut lamina propria. Nature *501*, 112–115.

Whittaker, E., Goldblatt, D., McIntyre, P., and Levy, O. (2018). Neonatal immunization: rationale, current state, and future prospects. Front. Immunol. *9*, 532.

Wiehe, K., Bradley, T., Meyerhoff, R.R., Hart, C., Williams, W.B., Easterhoff, D., Faison, W.J., Kepler, T.B., Saunders, K.O., Alam, S.M., et al. (2018). Functional Relevance of Improbable Antibody Mutations for HIV Broadly Neutralizing Antibody Development. Cell Host Microbe *23*, 759–765.e6.

Wiehe, K., Easterhoff, D., Luo, K., Nicely, N.I., Bradley, T., Jaeger, F.H., Dennison, S.M., Zhang, R., Lloyd, K.E., Stolarchuk, C., et al. (2014). Antibody light-chain-restricted recognition of the site of immune pressure in the RV144 HIV-1 vaccine trial is phylogenetically conserved. Immunity *41*, 909–918.

Willems, F., Vollstedt, S., and Suter, M. (2009). Phenotype and function of neonatal DC. Eur. J. Immunol. *39*, 26–35.

Williams, W.B., Liao, H.X., Moody, M.A., Kepler, T.B., Alam, S.M., Gao, F., Wiehe, K., Trama, A.M., Jones, K., Zhang, R., et al. (2015). Diversion of HIV-1 vaccine-induced immunity by gp41-microbiota cross-reactive antibodies. Science *349*, aab1253.

Williams, W.B., Zhang, J., Jiang, C., Nicely, N.I., Fera, D., Luo, K., Moody, M.A., Liao, H.X., Alam, S.M., Kepler, T.B., et al. (2017). Initiation of HIV neutralizing B cell lineages with sequential envelope immunizations. Nat. Commun. *8*, 1732.

Williams, W.B., Han, Q., and Haynes, B.F. (2018). Cross-reactivity of HIV vaccine responses and the microbiome. Curr. Opin. HIV AIDS *13*, 9–14.

Williams, W.B., Zhang, J., Jiang, C., Nicely, N.I., Fera, D., Luo, K., Moody, M.A., Liao, H.X., Alam, S.M., Kepler, T.B., et al. (2017). Initiation of HIV neutralizing B cell lineages with sequential envelope immunizations. Nat Commun *8*, 1732.

Willinger, T., Freeman, T., Herbert, M., Hasegawa, H., McMichael, A.J., and Callan, M.F.C. (2006). Human naive CD8 T cells down-regulate expression of the WNT pathway transcription factors lymphoid enhancer binding factor 1 and transcription factor 7 (T cell factor-1) following antigen encounter in vitro and in vivo. J. Immunol. *176*, 1439–1446.

Wright, P.F., Karron, R.A., Belshe, R.B., Thompson, J., Crowe, J.E., Jr., Boyce, T.G., Halburnt, L.L., Reed, G.W., Whitehead, S.S., Anderson, E.L., et al. (2000). Evaluation of a live, cold-passaged, temperature-sensitive, respiratory syncytial virus vaccine candidate in infancy. J. Infect. Dis. *182*, 1331–1342.

Wu, X., Wang, C., O'Dell, S., Li, Y., Keele, B.F., Yang, Z., Imamichi, H., Doria-Rose, N., Hoxie, J.A., Connors, M., et al. (2012). Selection pressure on HIV-1 envelope by broadly neutralizing antibodies to the conserved CD4-binding site. J Virol *86*, 5844–5856.

Yamadori, T., Baba, Y., Matsushita, M., Hashimoto, S., Kurosaki, M., Kurosaki, T., Kishimoto, T., and Tsukada, S. (1999). Bruton's tyrosine kinase activity is negatively regulated by Sab, the Btk-SH3 domain-binding protein. Proc. Natl. Acad. Sci. USA *96*, 6341–6346.

Yang, Z.F., Ho, D.W., Lau, C.K., Lam, C.T., Lum, C.T., Poon, R.T.P., and Fan, S.T. (2005). Allograft inflammatory factor-1 (AIF-1) is crucial for the survival and pro-inflammatory activity of macrophages. Int. Immunol. *17*, 1391–1397.

Zhang, R., Verkoczy, L., Wiehe, K., Munir Alam, S., Nicely, N.I., Santra, S., Bradley, T., Pemble, C.W., 4th, Zhang, J., Gao, F., et al. (2016). Initiation of immune tolerance-controlled HIV gp41 neutralizing B cell lineages. Sci. Transl. Med. *8*, 336ra62.

Zheng, G.X.Y., Terry, J.M., Belgrader, P., Ryvkin, P., Bent, Z.W., Wilson, R., Ziraldo, S.B., Wheeler, T.D., McDermott, G.P., Zhu, J., et al. (2017). Massively parallel digital transcriptional profiling of single cells. Nat. Commun. *8*, 14049.

Zhu, F., Xu, W., Xia, J., Liang, Z., Liu, Y., Zhang, X., Tan, X., Wang, L., Mao, Q., Wu, J., et al. (2014). Efficacy, safety, and immunogenicity of an enterovirus 71 vaccine in China. N. Engl. J. Med. *370*, 818–828.

STAR★METHODS

KEY RESOURCES TABLE

REAGENT or RESOURCE	SOURCE	IDENTIFIER
Antibodies		
Mouse anti-Human PD-1 Brilliant Violet 421, Clone EH12.2H7	Biolegend	Cat# 329920; RRID:AB_10960742
Live/Dead Fix Aqua	Thermo Fisher Scientific	L34957
Mouse anti-Human CD8a Brilliant Violet 570, Clone RPA-T8	Biolegend	Cat# 301038; RRID:AB_2563213
Rat anti-Human* CCR7 Brilliant Violet 605, Clone 3D12	BD Biosciences	Cat# 563711; RRID:AB_2738385
Mouse anti-Human CD25 Brilliant Violet 650, Clone BC96	Biolegend	Cat# 302634; RRID:AB_2563807
Mouse anti-Human CD4 Brilliant Violet 711, Clone OKT4	Biolegend	Cat# 317440; RRID:AB_2562912
Mouse anti-Human CD45RA Brilliant Violet 786, Clone 5H9	BD Biosciences	Cat# 741010; RRID:AB_2740633
Armenian Hamster anti-human ICOS BB515, Clone C398.4A	BD Biosciences	Cat# 565880; RRID:AB_2744480
Mouse anti-Human CCR6 BB700, Clone 11A9	BD Biosciences	Cat# 566477; RRID:AB_2744303
Mouse anti-Human Bcl-6 PE, Clone K112-91	BD Biosciences	Cat# 561522; RRID:AB_10717126
Mouse anti-Human CD183 PE-CF594, Clone 1C6/CXCR3	BD Biosciences	Cat# 562451; RRID:AB_11153118
Mouse anti-Human CD69 PE-Cy5, Clone FN50	Biolegend	Cat# 310908; RRID:AB_314843
Mouse anti-Human CD185 PE-Cy7, Clone MU5UBEE	eBioscience (Thermo Fisher Scientific)	Cat# 25-9185-42; RRID:AB_2573540
Rat anti-Human Foxp3 APC, Clone PCH101	eBioscience (Thermo Fisher Scientific)	Cat# 17-4776-42; RRID:AB_1603280
Mouse anti-Human Ki-67 Alexa Fluor 700, Clone B56	BD Biosciences	Cat# 561277; RRID:AB_10611571
Mouse anti-human CD3 APC-Cy7, Clone SP34-2	BD Biosciences	Cat# 557757; RRID:AB_396863
Live/Dead Fix Aqua	Thermo Fisher Scientific	L34957
Mouse anti-Human IgM Brilliant Violet 605, Clone G20-127	BD Biosciences	Cat# 562977; RRID:AB_2737928
Mouse anti-Human CD16 Brilliant Violet 650, Clone 3G8	Biolegend	Cat# 302036; RRID:AB_2632790
Mouse anti-Human CD3 Brilliant Violet 650, Clone SP34-2	BD Biosciences	Cat# 563916; RRID:AB_2738486
Mouse anti-Human CD14 Brilliant Violet 650, Clone M5E2	BD Biosciences	Cat# 563419; RRID:AB_2744286
Mouse anti-Human CD27 Brilliant Violet 711, Clone O323	Biolegend	Cat# 302834; RRID:AB_2563809
Mouse anti-Human CD20 Brilliant Violet 785, Clone 2H7	Biolegend	Cat# 302356; RRID:AB_2566316
Mouse anti-Human CD38 FITC, Clone OKT10	Caprico Biotechnologies	Cat# 100815
Mouse anti-Human CD72 PerCP, Clone Bu40	Novus Biologicals	Cat# NB100-64350PCP
Mouse anti-Human Bcl6 PE, Clone K112-91	BD Biosciences	Cat# 561522; RRID:AB_10717126
Mouse anti-Human CD1c PE-Dazzle594, Clone L161	Biolegend	Cat# 331532; RRID:AB_2565293
Mouse anti-Human CD69 PE-Cy5, Clone FN50	Biolegend	Cat# 310908; RRID:AB_314843
Mouse anti-Human CD21 PE-Cy7, Clone B-ly4	BD Biosciences	Cat# 561374; RRID:AB_10681717
Mouse anti-Human Ki67 Alexa Fluor 700, Clone B56	BD Biosciences	Cat# 561277; RRID:AB_10611571
Mouse anti-Human IgG APC-H7, Clone G18-145	BD Biosciences	Cat# 561297; RRID:AB_10611877

(*Continued on next page*)

Continued

REAGENT or RESOURCE	SOURCE	IDENTIFIER
CH106	Isolated from patient (Liao et al., 2013)	N/A
Goat Anti-Rhesus IgG(H+L)-FITC	Southern Biotech	Cat# 6200-02; RRID:AB_2796265
RD1-conjugated anti-p24	KC57, Beckman Coulter	Cat# 6604667; RRID:AB_1575989
CD14 (BV570)	Biolegend	Cat# 301832; RRID:AB_2563629
CD16 (PE-Cy7)	BD Biosciences	Cat# 557744; RRID:AB_396850
CD3 (PerCP Cy5.5)	BD Biosciences	Cat# 552852; RRID:AB_394493
CD20 (FITC),	BD Biosciences	Cat# 347673; RRID:AB_400338
CD27 (APC-Cy7)	Biolegend	Cat# 302816; RRID:AB_571977
IgD (PE)	Southern Biotech	Cat# 2030-09; RRID:AB_2795630
Bacterial and Virus Strains		
HIV-1 strain CH505TF, GENBANK: KC247556	Isolated from patient (Liao et al., 2013)	N/A
HIV-1 strain CH505.w4.3, GENBANK: KC247557	Isolated from patient (Liao et al., 2013)	N/A
HIV-1 strain MW965.26, GENBANK: U08455	Isolated from patient (Gao et al., 1996)	N/A
HIV-1 strain SF162.LS, GENBANK: EU123924	Isolated from patient (Liao et al., 2013)	N/A
HIV-1 strain 6644.V2.C33, GENBANK: HM215336	Isolated from patient (Gnanakaran et al., 2010)	N/A
HIV-1 strain DJ263.8, GENBANK: EU855130	Isolated from patient (Li et al., 2007)	N/A
HIV-1 strain 45_01dG5, GENBANK: JQ609687	Isolated from patient (Wu et al., 2012)	N/A
HIV-1 strain JR-FL, GENBANK: AY669728	Isolated from patient (Binley et al., 2004)	N/A
HIV-1 strain Q842.D12, GENBANK: AF407160	Isolated from patient (Long et al., 2002)	N/A
HIV-1 strain 57128.vrc15, AY736829	Isolated from patient (Long et al., 2002)	N/A
HIV-1 strain YU2, GENBANK: M93258	Isolated from patient (Li et al., 1992)	N/A
HIV-1 strain ZM17635F.66	Undetermined	N/A
HIV-1 strain Q168.A2, GENBANK: AF407148	Isolated from patient (Long et al., 2002)	N/A
HIV-1 strain BG1168.1, GENBANK: AY835443	Isolated from patient (Li et al., 2005)	N/A
Murine Leukemia virus: SVA-MLV	Negative Control Virus	NIH AIDS Reagent Program: catalog# 1065
HIV-1 strain CNE55, GENBANK HM215418	Isolated from patient (Gnanakaran et al., 2010)	N/A
HIV-1 strain TRO.11, GENBANK AY835445	Isolated from patient (Li et al., 2005)	N/A
HIV-1 strain SC422661.8, GENBANK AY835441	Isolated from patient (Li et al., 2005)	N/A
MuLV + Kifunensine	this paper	N/A
HIV-1 strain JR-FL + Kifunensine	JR-FL + Kifunensine (Doores and Burton, 2010)	N/A
HIV-1 strain JR-FL.ADIR.4 + Kifunensine	JR-FL mutant + Kifunensine (Saunders et al., 2017)	N/A

(*Continued on next page*)

Continued

REAGENT or RESOURCE	SOURCE	IDENTIFIER
HIV-1 strain JR-FL.GAIR.4 + Kifunensine	JR-FL mutant + Kifunensine (Saunders et al., 2017)	N/A
HIV-1 strain JR-FL.GDAR.2 + Kifunensine	JR-FL mutant + Kifunensine (Saunders et al., 2017)	N/A
HIV-1 strain JR-FL.GDIA.3 + Kifunensine	JR-FL mutant + Kifunensine (Saunders et al., 2017)	N/A
HIV-1 strain JR-FL.GAIA.4 + Kifunensine	JR-FL mutant + Kifunensine (Saunders et al., 2017)	N/A
Biological Samples		
Plasma and PBMCs from macaques in study no.1+A80:C82	this paper	
Plasma and PBMCs from macaques in study no.2	this paper	
Plasma and PBMCs from macaques in study no.3	this paper	
Chemicals, Peptides, and Recombinant Proteins		
soluble CD4	NIH AIDS Repository	Cat #4615
Expi293 media	Invitrogen	Cat #A1435102
Expifectamine	Life Technologies	Cat #A14524
Protein A beads	Pierce	Cat #PI-20334
Vivaspin 15	Sartorius Stedim	Cat #VS15T22
Vivaflow 50	Sartorius Stedim	Cat #VF05P2
AmpliTaq Gold 360 Mastermix	Applied Biosystems by Thermo Fisher Scientific	Cat #4398881
d7_HIV_gp120_CH0505 T/F_Atb_SavAF647	Williams et al., 2017	N/A
d7_HIV_gp120_CH0505 T/F_Atb_SavBV421	Williams et al., 2017	N/A
d7_HIV_gp120_CH0505 T/F_Atb_SavAF647	Williams et al., 2017	N/A
d7_HIV_gp120_CH0505 T/F_Atb_SavBV421	Williams et al., 2017	N/A
CH505_TF D7 gp120/293F/Mon	Williams et al., 2017	N/A
CH0505 TF gp120 d371I	Williams et al., 2017	N/A
ch505TF SOSIP 664 v4.1	Saunders et al., 2017a	N/A
ch505wk100 SOSIP 664 v4.1	Saunders et al., 2017a	N/A
Experimental Models: Cell Lines		
Human cell line TZM-bl	NIH ARRRP	Cat #8129
Human cell line Expi293F	Invitrogen	Cat #14527
monocytic THP-1 cell line	ATCC	Cat #TIB-202
CEM.NKRCCR5 cells	NIH AIDS Repository	Cat # 4376
Recombinant DNA		
pcDNA3.1/hygromycin (+)	Invitrogen	Cat # V87020
Software and Algorithms		
Diva	BD Biosciences	N/A
FlowJo (version 9.9.4)	FlowJo, LLC	N/A
GraphPad Prism (version 7.0)	GraphPad Software	N/A
CellRanger	Zheng et al., 2017	N/A
Seurat	Satija et al., 2015	N/A
SAS v9.4	SAS Institute	N/A
Cloanalyst Program	Kepler, 2013	N/A
QIIME v. 1.9.1	Caporaso et al., 2010	N/A
vsearch v. 1.11.1	Rognes et al., 2016	N/A
LEfSe (Linear discriminant analysis effect size)	Segata et al., 2011	N/A

LEAD CONTACT AND MATERIALS AVAILABILITY

Further information and requests for resources and reagents should be directed to and will be fulfilled by the Lead Contact, Barton F. Haynes (barton.haynes@duke.edu). This study did not generate new unique reagents. There are no restrictions to the availability of data generated in this study.

EXPERIMENTAL MODEL AND SUBJECT DETAILS

All rhesus macaques (*Macaca mulatta*) were housed indoors at the California National Primate Research Center (CNPRC), CA or Bioqual, Rockville, MD, and were maintained in accordance with the Association for Assessment and Accreditation of Laboratory Animals with the approval of the Animal Care and Use Committees of the UC Davis. Research was conducted in compliance with the Animal Welfare Act and other federal statutes and regulations relating to animals and experiments involving animals and adheres to principles stated in the Guide for the Care and Use of Laboratory Animals, NRC Publication, 2011 edition. The neonatal macaques were dam-reared, and were up to 7 days of age at the time of the first immunization. Dam-reared neonatal macaques were selected because it is most natural, and because it was previously shown that nursery-reared neonatal macaques have differences in microbiome and immune function (Ardeshir et al., 2014; Narayan et al., 2015). Study approval: All animal experiments performed in this study were approved by the Duke, University of California, Davis and Bioqual IACUCs. The term neonatal macaques was used to denote macaques that received their initial immunizations beginning from birth to one week of life.

Vaccine Regimens and Study Groups

CH505 transmitted-founder (T/F), week53, week78 and week100 gp120 Env-variants were administered in sequential combinations in GLA/SE (IDRI) in 4 neonatal macaques [2 females (45405 and 45423) and 2 males (45404 and 45425)] and 4 adult macaques (all males) for a total of 8 and 6 immunizations, respectively, in Study no. 1. CH505 T/F (3 times), week53, week78 and week100 sequential CH505 gp140 SOSIPs were administered in sequential combinations in GLA/SE in 3 neonatal macaques [2 females (179059 and 178951) and 1 male (177890)] and 4 adult macaques [3 females (150799, T270, T274) and 1 male (150129)] for a total of 6 immunizations in Study no. 2. CH505 T/F gp145 DNA (2 times) and CH505 T/F, week53, week78 and week100 sequential CH505 gp140 v4.1 SOSIP were administered in sequential combinations in Poly ICLC (Hiltonol®, Oncovir) in 2 neonatal macaques [1 female (177715) and 1 male (178122)] and 4 adult macaques [3 females (T241, T243, 177850) and 1 male (177811)] for a total of 6 immunizations in Study no. 3. Stabilized CH505 SOSIPs contained E64K and A316W trimer stabilization mutations (Saunders et al., 2017a; de Taeye et al., 2015).

Immunizations were administered intramuscular in the leg of each animal with a total of 50μg (neonatal macaques) or 100 μg (adult macaques) of total CH505 proteins. When necessary, adult animals were immobilized with ketamine HCl (10 mg/kg) administered intramuscularly; when feasible, neonatal macaques were handheld for the procedures and sample collections. Blood samples were collected via venipuncture at 2 weeks after each immunization. Stool was collected from the cage pan, or from the neonate when it was handheld. Vaccine-induced Ab repertoires were studied 2 weeks after 4^{th} and 6^{th} immunizations in plasma and blood-derived memory B cells of four neonatal macaques immunized with CH505 gp120s.

METHOD DETAILS

Flow Cytometry Memory B Cell Sorting

B cell sorting was performed using flow cytometry approaches as described (Wiehe et al., 2014; Zhang et al., 2016). Briefly, peripheral blood mononuclear cells (PBMCs) of immunized macaques were stained with AquaVital dye, CD14 (BV570), CD16 (PE-Cy7), CD3 (PerCP Cy5.5), CD20 (FITC), CD27 (APC-Cy7), and IgD (PE). Single-cell isolation of memory B cells (AquaVital dye$^-$, CD14$^-$, CD16$^-$, CD3$^-$, IgD$^-$, CD20$^+$) stained with both AlexaFluor 647 and Brilliant Violet 421–tagged HIV-1 CH505 T/F gp120 proteins (CH505 double positives), and cells stained with BV421-tagged CH505 T/F gp120, but not AF647-tagged CH505 T/F gp120 Δ371 mutant protein (CH505 single positives) was performed using a fluorescence-activated cell sorter FACSAria II (BD Biosciences, San Jose, CA), and the flow cytometry data were analyzed using FlowJo (Treestar, Ashland, OR).

Phenotypic Analysis by Flow Cytometry

Macaque PBMCs were stained by a panel of markers, including CD38, Bcl-6, CD1c, CD69, CD21, Ki67, IgG, IgM, CD3/CD14/CD16, CD27, and CD20 to discriminate various B cell subsets. B cells (AquaVital dye$^-$, CD14$^-$, CD16$^-$, CD3$^-$, CD20$^+$) stained with both AlexaFluor 647 and Brilliant Violet 421-tagged HIV-1 CH505 T/F gp120 proteins or CH505 T/F stabilized SOSIP proteins were defined as gp120-specific or SOSIP-specific B cells. For the T cell subsets, a panel of markers including ICOS, CCR6, Bcl-6, CD183, CD69, CD185, Foxp3, Ki-67, CD3, PD-1, CD8a, CCR7, CD25, CD4 and CD45RA was used. Aqua Vital Dye was used to distinguish live from dead cells (Invitrogen).

Ab Binding Specificities and Epitope Mapping

Plasma Abs and recombinant mAbs were screened for binding specificities to multiclade HIV-1 Envs by means of standard ELISA as described (Tomaras et al., 2008). We isolated candidate CD4bs mAbs and non-CD4bs mAbs as previously described (Williams et al.,

2017). Plasma Abs were tested for epitope specificity by peptide microarray as described (Shen et al., 2015; Tomaras et al., 2011). Linear peptides (15-mers overlap by 12) from vaccine-strain and consensus Env gp120 was used in this analysis. Additionally, we mapped Ab epitope for plasma and blood-derived mAbs via competitive inhibition assay in ELISA (Zhang et al., 2016). For CD4 (binding site) blocking assays we used soluble CD4 (Progenics Pharm Inc.) or CH106 bnAb. CH65, HA influenza antibody, was used as a negative control binding antibody.

Antibody-Dependent Cellular Phagocytosis Assay

Antibody-dependent phagocytosis was assessed by the measurement of the uptake of antibody-opsonized, antigen-coated fluorescent beads by the monocytic THP-1 cell line (ATCC; #TIB-202) (Ackerman et al., 2011; Tay et al., 2016).

Plasma Binding to the Surface of HIV-1-Infected Cells

Indirect surface staining was used to measure the ability of NHP plasma samples to bind HIV-1 envelope expressed on the surface of infected cells as described (Bradley et al., 2017; Ferrari et al., 2011). CD4+ T cells (CEM.NKR.CCR5) infected with HIV-1 CH505TF was used as the effector cells (Howell et al., 1985; Lyerly et al., 1987; Trkola et al., 1999).

Neutralization Assays

Neutralization activity of Abs was measured in 96-well culture plates by using Tat-regulated luciferase (Luc) reporter gene expression to quantify reductions in virus infection in TZM-bl cells (Sarzotti-Kelsoe et al., 2014). Wild-type JR-FL and GDIR alanine mutant JR-FL viruses were produced in kifunensine-treated cells (Saunders et al., 2017b). HIV-1 B.JR-FL produced in the presence of kifunensine (KIF-JRFL), a glycosylation pathway inhibitor that results in a high density of $Man_9GlcNAc_2$ glycans was previously described (Doores and Burton, 2010; Scanlan et al., 2007). For plasma tested in neutralization, the starting dilutions for neonatal macaques 177890, 178951 and 179059 were 1:100, 1:50 and 1:100 due to limited samples; all other samples were tested at starting dilution of 1:20. Neutralization sensitivity of HIV-1 strains: easy-to-neutralize (tier 1) and difficult-to-neutralize (tier 2).

PCR Isolation of Heavy and Light Chain Genes

Heavy (IGHV) and light (IGKV, IGLV) chain genes were amplified as described previously (Liao et al., 2009). The PCR-amplified genes were then purified and sequenced with 4 μM of forward and reverse primers. Sequences were analyzed by using the macaque library in Clonalyst, such as the VDJ arrangements of the immunoglobulin IGHV, IGKV, and IGLV sequences, somatic mutations, and CDR3 length (Kepler, 2013; Wiehe et al., 2014). Sequences were subject to statistical analysis for lineage membership as described (Williams et al., 2015).

Transient and Recombinant Ab Expression

Transient and recombinant Ab expressions were performed as described (Liao et al., 2009, 2011; Wiehe et al., 2014). Briefly, an aliquot of the purified PCR amplicon was used for overlapping PCR to generate a linear expression cassette. The expression cassette was transfected with ExpiFectamine (Thermo Fisher Scientific) into 293T cells. The supernatant containing recombinant Abs were used for binding assays. The genes of selected heavy chains and kappa/lambda chains were synthesized as IgG1 and cloned into pcDNA3.1 plasmid (GenScript). Recombinant Ab expressions and purification were performed as described (Liao et al., 2011; Wiehe et al., 2014).

Single-Cell RNA Sequencing of Rhesus Macaque PBMCs

PBMCs from neonatal and adult macaques (macaque 150129 not included) immunized with CH505 SOSIPs in **Study no.2** at week 9 (post 2 immunizations) were used. We also studied PBMCs from one neonatal macaque (177715) and one adult macaque (T243) from **Study no. 3** at week 6 (post 2 immunizations). PBMCs were thawed, washed and placed in single-cell suspensions with PBS + 0.04% BSA. Cellular suspensions were loaded on a GemCode Single-Cell instrument (10X Genomics, Pleasanton, CA) to generate single-cell beads in emulsion (Zheng et al., 2017). Single-cell RNA-seq libraries were then prepared using a GemCode Single Cell 3′ Gel bead and library kit (10X Genomics). Single-cell barcoded cDNA libraries were quantified by quantitative PCR (Kappa Biosystems, Wilmington, MA) and sequenced on an Illumina NextSeq 500 (San Diego CA). Read lengths were 26 bp for read 1, 8 bp i7 index, and 98 bp read 2. Cells were sequenced to greater than 50,000 reads per cell. The Cell Ranger Single Cell Software Suite was used to perform sample de-multiplexing, barcode processing and single-cell 3′ gene counting (Zheng et al., 2017). Reads were aligned to macaque genome assembly, Mmul_8.0.1. from the Ensemble (http://ensemble.org) (Dobin et al., 2013; Zheng et al., 2017). We could not identify high expression of CD4 transcript in T cells, which may indicate disparate expression of the transcript and surface protein or polymorphisms in the CD4 transcript that hinder alignment of transcript reads to the genome reference. Graph based cell clustering, dimensionality reduction and data visualization were analyzed by the Seurat R package (Satija et al., 2015). Cells that exhibited high transcript counts, > 0.1% mitochondrial transcripts were excluded from analysis. Differentially expressed transcripts were determined in the Seurat R package utilizing the Likelihood-ratio test for single cell gene expression statistical test (McDavid et al., 2013). Graphics were generated using the Seurat and ggplot2 R packages. Four known cell types were identified within PBMCs on the tSNE plot representation by expression of markers used to define the clusters – CD19 and/or CD20, B cells; CD3D, T cells; NCR1, NK cells; LYZ and CD14, Monocytes.

Microbiome Analysis

The V4 region of the 16S gene was amplified with primers 515FB/806RB following protocols of the Illumina 16S amplicon protocols of the Earth Microbiome Project (http://press.igsb.anl.gov/earthmicrobiome/protocols-and-standards/16s/). Sequencing was performed using 150 bp paired end Illumina MiSeq sequencing. The obtained 16,318,607 paired reads were merged with fastq-join [1], yielding 13,727,040 assembled 16S amplicon sequences. Subsequent quality filtering and demultiplexing was performed with split_libraries_fastq.py of QIIME v. 1.9.1 (Caporaso et al., 2010), setting a minimal Phred quality score of 20. These settings resulted into 12,549,251 filtered amplicons, with a median length of 253 bp, which were used for downstream analysis. During further processing with vsearch v. 1.11.1 (Rognes et al., 2016), amplicon sequences were dereplicated, filtered for chimeras, and clustered at a 97% identity threshold into 89,268 operational taxonomic units (OTUs). Subsequent taxonomic assignment against the 16S reference sequence set of SILVA, v. 1.28 (Quast et al., 2013), OTU sequence alignment and generation of an unrooted phylogenetic tree, was performed in QIIME. A basic statistical diversity analysis was performed, using core_diversity_analysis.py of QIIME, including alpha-, beta-diversity, and relative taxa abundances in sample groups. The determined relative taxa abundances were further analyzes with LEfSe (Linear discriminant analysis effect size) (Segata et al., 2011), to identify differential biomarkers in sample groups. Alpha diversity analysis was performed on samples after rarefaction to 10000 sequences/sample (minimum sampling depth). Rarefaction curves were generated for the phylogenetic distance between two groups. Phylogenetic distance were calculated at a rarefaction depth of 10000 sequences per sample.

QUANTIFICATION AND STATISTICAL ANALYSIS

Exact Wilcoxon test was performed to compare differences in mAbs from neonatal and adult macaques with p value < 0.05 considered significant. Likelihood ratio test was performed to analyze the differentially expressed transcripts with p value < 0.05 considered significant. Nonparametric analyses of longitudinal data (R package nparLD) were performed to test the hypothesis that there exist differences between groups across time (p value < 0.05 considered significant) (Noguchi et al., 2012). This method was used to answer two questions for repeated-measures on the same subjects: 1) Are the age group effects similar over time/Are the age group profiles parallel?; 2) Do the groups have the same effect/ Do the groups have coincident profiles? This statistical method does not require distributional assumptions and allows for the assessment of interaction terms even with a small sample size. Due to the small sample size within SOSIP immunized animals in **Studies nos. 2 and 3**, we could not conduct a stratified statistical analyses and thus combined these groups for comparisons.

DATA AND CODE AVAILABILITY

The single-cell RNA seq unprocessed reads have been deposited in the NCBI SRA database under the accession number PRJNA555837. Code and other processed file formats are available from corresponding authors upon reasonable request. The data presented in this manuscript are tabulated in the main paper and in the supplementary materials. Research materials used in this study are available from Duke University upon request and subsequent execution of an appropriate materials transfer agreement.